*J Neurophysiol* 90: 271–290, 2003;
10.1152/jn.01074.2002.

# Brain Stem Pursuit Pathways: Dissociating Visual, Vestibular, and Proprioceptive Inputs During Combined Eye-Head Gaze Tracking

**Jefferson E. Roy and Kathleen E. Cullen**

*Aerospace Medical Research Unit, Department of Physiology, McGill University, Montreal, Quebec H3G 1Y6, Canada*

Submitted 27 November 2002; accepted in final form 6 March 2003

**Roy, Jefferson E. and Kathleen E. Cullen.** Brain stem pursuit pathways: dissociating visual, vestibular, and proprioceptive inputs during combined eye-head gaze tracking. *J Neurophysiol* 90: 271–290, 2003; 10.1152/jn.01074.2002. Eye-head (EH) neurons within the medial vestibular nuclei are thought to be the primary input to the extraocular motoneurons during smooth pursuit: they receive direct projections from the cerebellar flocculus/ventral paraflocculus, and in turn, project to the abducens motor nucleus. Here, we recorded from EH neurons during head-restrained smooth pursuit and head-unrestrained combined eye-head pursuit (gaze pursuit). During head-restrained smooth pursuit of sinusoidal and step-ramp target motion, each neuron's response was well described by a simple model that included resting discharge (bias), eye position, and velocity terms. Moreover, eye acceleration, as well as eye position, velocity, and acceleration error (error = target movement − eye movement) signals played no role in shaping neuronal discharges. During head-unrestrained gaze pursuit, EH neuron responses reflected the summation of their head-movement sensitivity during passive whole-body rotation in the dark and gaze-movement sensitivity during smooth pursuit. Indeed, EH neuron responses were well predicted by their head- and gaze-movement sensitivity during these two paradigms across conditions (e.g., combined eye-head gaze pursuit, smooth pursuit, whole-body rotation in the dark, whole-body rotation while viewing a target moving with the head (i.e., cancellation), and passive rotation of the head-on-body). Thus our results imply that vestibular inputs, but not the activation of neck proprioceptors, influence EH neuron responses during head-on-body movements. This latter proposal was confirmed by demonstrating a complete absence of modulation in the same neurons during passive rotation of the monkey's body beneath its neck. Taken together our results show that during gaze pursuit EH neurons carry vestibular- as well as gaze-related information to extraocular motoneurons. We propose that this vestibular-related modulation is offset by inputs from other premotor inputs, and that the responses of vestibuloocular reflex interneurons (i.e., position-vestibular-pause neurons) are consistent with such a proposal.

## INTRODUCTION

In the head-restrained condition, primates generate smooth eye movements, termed smooth pursuit, to follow a slowly moving target. A number of parallel and interconnected pathways are involved in initiating and maintaining smooth-pursuit eye movements (for review, see Keller and Heinen 1991); however, particular importance has been assigned to the cortico-ponto-cerebellar pathway arising from the medial superior temporal sulcus (MST) of the extrastriate cortex. This pathway accesses the brain stem circuitry via inhibitory projections from the ipsilateral cerebellar flocculus and ventral paraflocculus, herein referred to as the floccular lobe (Balaban et al. 1981; Dow 1937; Gerrits and Voogd 1989; Langer et al. 1985). Under more natural conditions (i.e., when the head is not restrained), humans and primates use coordinated movements of the head as well as the eyes, referred to as gaze pursuit, to align their axis of gaze (gaze = eye-in-head position + head-in-space position) with a moving target. Only a handful of investigations have studied how structures in the cortico-ponto-cerebellar pursuit pathway respond during these combined eye-head movements.

The overall goal of the present study was to determine what signals are carried by the brain stem premotor pursuit pathway during head-restrained and combined eye-head pursuit. The brain stem neurons in the rostral-medial and ventral-lateral vestibular nuclei, which receive direct projections from the floccular lobe, have been termed flocculus target neurons (FTN) (Broussard and Lisberger 1992; Lisberger and Pavelko 1988; Lisberger et al. 1994a,b). The responses of these brain stem neurons largely correspond with those of a distinct physiological subclass of cells, termed eye-head (EH) neurons, which have been well characterized during eye and head movements in the head-restrained monkey (Chen-Huang and McCrea 1999; Cullen at al. 1993; Gdowski and McCrea 1999, 2000; Gdowski et al. 2001; McCrea et al. 1996; McFarland and Fuchs 1992; Scudder and Fuchs 1992; Tomlinson and Robinson 1984). Accordingly, for the sake of simplicity, both FTN and EH neurons will be referred to from here on as EH neurons (although these 2 populations of neurons may not be strictly equivalent). EH neurons are thought to be the most significant premotor input to the extraocular motoneurons of the abducens nucleus during smooth pursuit eye movements (Cullen at al. 1993; Lisberger et al. 1994a,b; McFarland and Fuchs 1992; Scudder and Fuchs 1992).

To date, much is known about the signals carried by cerebellar neurons that project to EH neurons (i.e., Purkinje cells of the floccular lobe) during head-restrained smooth pursuit. The discharges of these cells can be considered with respect to their two sources of input, namely climbing fibers and mossy fibers. Inputs from the climbing fibers, which originate from the inferior olive (Eccles et al. 1966; Thach 1967), result in the complex spikes in the Purkinje cells (for review, see Bloedel and Courville 1981). The role of the climbing fiber input is still unclear (reviewed in Simpson et al. 1996), but many assume

Address for reprint requests: K. E. Cullen, Aerospace Medical Research Unit, 3655 Promenade Sir William Osler, Montreal, Quebec H3G 1Y6, Canada (E-mail: kathleen.cullen@mcgill.ca).

The costs of publication of this article were defrayed in part by the payment of page charges. The article must therefore be hereby marked "*advertisement*" in accordance with 18 U.S.C. Section 1734 solely to indicate this fact.

that it functions to modify the efficacy of the synapse between mossy fibers and Purkinje cell. Moreover there is evidence that in rabbit (Frens et al. 2001; Graf et al. 1988) and monkey (Kahlon and Lisberger 2000; Stone and Lisberger 1990b) complex spike trains encode performance errors (i.e., retinal slip).

Mossy fiber inputs are responsible for the simple spike activity of Purkinje cells (for review, see Stone and Lisberger 1990a). Because simple spikes occur much more frequently (discharges rates reaching ≤300 spikes/s) as compared with complex spike activity (~1 spikes/s), it seems likely that the information carried to the brain stem by simple spikes would govern, for the most part, the response profiles of EH neurons. During smooth pursuit, simple spike trains, in contrast to complex spikes, chiefly encode eye position, eye velocity, and, to a much smaller degree, eye acceleration (Leung et al. 2000; Suh et al. 2000). Whether simple spike trains also encode visual error signals remains controversial. On the one hand, it has been proposed that simple spike activity in monkey can encode relatively small, albeit significant, retinal velocity and acceleration error information during sinusoidal optokinetic stimulation (Hirata and Highstein 2001) as well as velocity error information when unpredictable changes in target direction are applied during pursuit (Suh et al. 2000). On the other hand, Kahlon and Lisberger (2000) have suggested that transient responses of simple spikes during pursuit initiation reflect the influence of feed-forward image motion.

It is not yet known if EH neuron responses encode error-related information (position, velocity, and acceleration) or eye-acceleration signals during smooth pursuit. For example, EH neurons could potentially receive visual error signals from either Purkinje cells within the floccular lobe or via direct projections from midbrain structures such as the accessory optic system and/or the nucleus of the optic tract that encode visual-slip information (Kato et al. 1995; Wylie and Linkenhoker 1996). Prior characterizations of brain stem EH neurons during head-restrained pursuit have focused on only the eye position and eye-velocity-related response of these neurons during sinusoidal smooth pursuit (Cullen et al. 1993; Lisberger et al. 1994a,b; McFarland and Fuchs 1992; Scudder and Fuchs 1992). Hence, the first specific goal of this study was to determine which eye-movement-based and/or error-based model best describes the discharge dynamics of EH neurons during smooth-pursuit eye movements made in the head-restrained condition.

In the head-unrestrained condition, when coordinated eye and head movements are made to pursue a target, at least three inputs could function to modify the responses of EH neurons. First, as noted in the preceding text, floccular lobe Purkinje cells send inhibitory projections to EH neurons. In the rhesus monkey, Purkinje cells encode head velocity during passive whole-body rotation where the monkey "cancels" its VOR by tracking a target that moves with the head (pWBRc) (Fukushima et al. 1999; Kahlon and Lisberger 2000; Lisberger and Fuchs 1978; Miles et al. 1980; Stone and Lisberger 1990a). These neurons have been termed gaze velocity Purkinje cells because they respond similarly to changes in the axis of gaze relative to space during pWBRc and head-restrained smooth pursuit. Accordingly, it has been proposed that they would send a gaze motor command rather than an eye motor command to the brain stem during combined eye-head gaze pursuit (Barnes 1993). In contrast, most floccular lobe Purkinje cells and presumably EH neurons in squirrel monkey, encode eye- rather than gaze-related signals during smooth pursuit, pWBRc, and head-unrestrained pursuit (Belton and McCrea 1999, 2000b). Thus it appears that rhesus monkeys have a much greater proportion of gaze velocity Purkinje cells as compared with squirrel monkeys (Fukushima et al. 1999; Lisberger and Fuchs 1978; Miles et al. 1980; Stone and Lisberger 1990). To date, no study has recorded the responses of rhesus floccular lobe Purkinje cells or EH neurons (in either species) during coordinated eye-head gaze pursuit. Accordingly, the second specific goal of the present study was to determine whether EH neurons encode an eye- or gaze-related motor command during coordinated eye-head gaze pursuit.

In addition to the floccular lobe projection, vestibular and proprioceptive inputs to the vestibular nuclei could further modify the responses of EH neurons during the head movements made during gaze pursuit. EH neurons are known to receive direct monosynaptic projections from the ipsilateral vestibular nerve (Broussard and Lisberger 1992; Chen-Huang and McCrea 1999; Gdowski and McCrea 1999, 2000; Scudder and Fuchs 1992) and polysynaptic projections from the contralateral vestibular nerve (Broussard and Lisberger 1992). Indeed, most EH neurons carry head-velocity-related signals during passive whole-body rotations in the dark. Moreover, neurons in regions of the vestibular nuclei that contain EH neurons receive inputs from neck muscle proprioceptors via a disynaptic pathway (Sato et al. 1997). The active head movements made during gaze pursuit would also activate neck proprioceptors and could in turn modulate EH neuron responses.

Prior work in decerebrate and/or anesthetized cat has demonstrated that passive activation of neck muscle proprioceptors can influence responses of neurons in the medial vestibular nuclei (Anastasopoulos and Megner 1982; Boyle and Pompeiano 1981; Wilson et al. 1990). Studies in alert squirrel monkey have suggested that most second-order neurons in the medial vestibular nuclei including EH neurons are influenced by passive activation of neck proprioceptors (Gdowski and McCrea 1999, 2000; Gdowski et al. 2001). In contrast, our recent studies in rhesus monkey have found no evidence that second-order neurons within the medial vestibular nuclei are influenced by neck proprioceptive inputs (Roy and Cullen 2001, 2002). These latter studies focused on two distinct classes of neurons in the medial vestibular nuclei, namely position-vestibular-pause and vestibular-only neurons, and did not consider EH neurons. Thus the third specific goal of the present study was to address whether and how vestibular and/or neck proprioceptors inputs influence EH neuron responses in rhesus monkey during the head-on neck movements made during gaze pursuit.

## METHODS

Three rhesus monkeys (2 *Macaca mulatta* and 1 *M. fasicularis*) were prepared for chronic extracellular recording using aseptic surgical techniques. All experimental protocols were approved by the McGill University Animal Care Committee and were in compliance with the guidelines of the Canadian Council on Animal Care.

### *Surgical procedures*

The surgical techniques were similar to those previously described by Roy and Cullen (2001, 2002). Briefly, an 18- to 19-mm diam eye

coil (3 loops of Teflon-coated stainless steel wire) was implanted on the right eye behind the conjunctiva. In addition, a dental acrylic implant was fastened to each animal's skull using stainless steel screws. The implant held in place a stainless steel post that was used to restrain the animal's head and a stainless steel recording chamber that was positioned to access the medial vestibular nucleus (posterior and lateral angles of 30°). During the surgery, isoflurane gas was utilized to initiate (2–3%) and maintain (0.8–1.5%) anesthesia. After the surgery, buprenorphine (0.01 mg/kg im) was utilized for postoperative analgesia, and monkeys were allowed to recover for 2 wk before commencing experimental sessions.

### *Data acquisition*

During each experiment, the monkey sat comfortably in a primate chair, which was placed on a vestibular turntable. With the monkey initially head-restrained, extracellular single-unit activity was recorded using enamel-insulated tungsten microelectrodes (7–10 MΩ impedance, Frederick-Haer) as has been described elsewhere (Roy and Cullen 2001, 2002). To determine the location of the medial and lateral vestibular nuclei, the location of the abducens nucleus was first identified based on its stereotypical discharge patterns during eye movements (Cullen et al. 1993; Sylvestre and Cullen 1999). Previous studies had shown that EH neurons are distributed between the vestibular nuclei and nucleus prepositus hypoglossi (Cullen at al. 1993; McFarland and Fuchs 1992). In the present study, single-unit recordings were for the most part limited to a small region of the brain stem extending 0.5–1.25 mm caudal to the abducens nucleus and 1.25–2.5 lateral of the midline, corresponding to the rostral-medial and ventral-lateral vestibular nuclei (McCrea et al. 1987; Tomlinson and Robinson 1984). Reconstructions of recording locations indicated that most neurons (38/42) were located within this area. Consistent with prior studies in rhesus (McFarland and Fuchs 1992; Scudder and Fuchs 1992), the anatomical distribution of these cell demonstrated considerable overlap with position-vestibular-pause and vestibular-only neurons. The remaining small percentage of neurons (i.e., $n = 4$, $<10\%$) were located in the most lateral aspect of the adjacent nucleus prepositus hypoglossi.

Gaze and head position were measured using the magnetic search-coil technique (Fuchs and Robinson 1966), and turntable velocity was measured using an angular velocity sensor (Watson). Unit activity, horizontal and vertical gaze and head positions, target position, and table velocity were recorded on DAT tape for later playback. Action potentials were discriminated off-line using a windowing circuit (BAK) that was manually set to generate a pulse coincident with the rising phase of each action potential. Gaze position, head position, target position, and table velocity signals were low-pass filtered at 250 Hz (8 pole Bessel filter) and sampled at 1,000 Hz.

### *Behavioral paradigms*

For a juice reward, monkeys were trained to follow a target light (HeNe laser) that was projected onto a cylindrical screen located 60 cm away from the monkey's head. Target and turntable motion, and on-line data displays were controlled by a UNIX-based real-time data-acquisition system (REX) (Hayes et al. 1982). The discharges of EH neurons were first characterized during a series of head-restrained paradigms. Neuronal responses during saccades and ocular fixation were recorded while the monkey attended to a target that stepped between horizontal positions over a range of ±30°. Neuronal sensitivities to smooth pursuit eye movements were determined using two different tasks: pursuit of sinusoidal (0.5 Hz, 80°/s peak velocity) target motion in the horizontal plane and pursuit of step-ramp target motion (Rashbass 1961). In this latter task, the monkey initially fixated a stationary target, which stepped to an eccentric position after a random fixation period (750–3,000 ms) and then began to move at a constant velocity of either 40 or 80°/s in the direction opposite to the step (Dubrovsky and Cullen 2002; Wellenius and Cullen 2000). A step size was chosen for each target velocity, which provided initial smooth eye movements that were not preceded by corrective saccades. Neuronal sensitivities to head movement during passive whole-body rotation (0.5 Hz, 40 and 80°/s peak velocity) were tested by rotating monkeys about an earth vertical axis in the dark (pWBRd) and while they cancelled their VOR by fixating a target that moved with the vestibular turntable (pWBRc).

After a neuron was fully characterized in the head-restrained condition, the monkey's head was slowly and carefully released allowing the monkey to rotate its head through the natural range of motion in the yaw (horizontal), pitch (vertical), and roll (torsional) axes. The waveform of the neuron was monitored to ensure that isolation was maintained. The response of the same neuron was then recorded during active head movements made during combined eye-head gaze shifts (15–65° in amplitude) and combined eye-head gaze pursuit of a sinusoidal target (0.5 Hz, 80°/s peak velocity) and a step-ramp target moving at a constant velocity of either 40 or 80°/s.

To determine whether the activation of neck proprioceptive input modulated neuronal discharges, EH cells were then recorded during two additional paradigms. First, the experimenter manually rotated the monkey's head to induce rapid motion of the head relative to a stationary body. Second, the monkey's head was held stationary relative to the earth while its body was passively rotated at 0.5 Hz at 40°/s peak velocity. Responses to rapid unexpected perturbations of the head were also recorded for a subset of neurons where either a short-duration (~40 ms), high-acceleration ($>10{,}000°/s^2$), and high-velocity (~100°/s) perturbation was applied to the head via a precision torque motor (Huterer and Cullen 2002) or the head was momentarily (~500 ms) braked using a magnetic clutch during step-ramp pursuit (Cullen et al. 1993).

### *Analysis of neuron discharges*

Analyses of neuronal discharges were performed using custom algorithms (Matlab, Mathworks). Recorded gaze- and head-position signals were digitally low-pass filtered using a 51st-order finite-impulse-response (FIR) filter with a Hamming window and cut-off frequency set to 125 Hz. Eye position was calculated from the difference between gaze- and head-position signals. Gaze-, eye-, and head-position signals were digitally differentiated to produce velocity signals. Neuronal firing rate was represented using a spike density function in which a Gaussian function (SD of 5 ms for saccades and gaze shifts and 10 ms for remainder of the paradigms) was convolved with the spike train (Cullen et al. 1996). Saccade and gaze shift onsets and offsets were defined using a ±20°/s gaze velocity criterion.

To quantify a neuron's response to eye position, a regression analysis was used to determine the relationship between mean eye position and mean neuronal firing rate during periods of steady fixation. This analysis yielded a resting discharge ($bias_x$, spikes/s) and an eye position sensitivity [$k_x$, (spikes/s)/°]. A least-squared regression analysis was also applied to neuronal discharges during saccades, smooth pursuit, passive whole body rotation in the dark and while fixating a target that moved with the animal, passive body-under-head (BUH) rotations, passive head-on-body rotations (PHBR), gaze shifts, gaze pursuit, and high-frequency perturbations of the head applied during steady eye fixation. The model formulations used to estimate the eye-, head-, and/or neck-movement sensitivities in each condition are described in RESULTS. To avoid fitting neuronal response as cells were driven into cut-off, only data for which the firing rate was >10 spikes/s was included in the optimization. For all behavioral paradigms, except for saccades and gaze shifts, only unit data from intervals between quick phases of vestibular nystagmus and/or gaze shifts and saccades were included in the analysis. During sinusoidal passive whole body rotation paradigms, neuronal phase relative to head velocity was calculated from the estimated head velocity and

acceleration sensitivities [phase = arctan (acceleration coefficient / velocity coefficient) * 180/Pi].

To quantify the ability of the linear regression analysis to model neuronal discharges, the variance-accounted-for (VAF) provided by each regression equation was determined. The VAF was computed as {1 – [var(est – fr)/var(fr)]}, where est represents the modeled firing rate (i.e., regression equation estimate) and fr represents the actual firing rate. The VAF provided a normalized measure of each model's goodness of fit that allowed comparisons across models and neurons. For example, a VAF of 0.5 would indicate that 50% of the variability in a unit's discharge is explained by the model, corresponding to a correlation coefficient ($R$) of 0.71 in a bivariate linear regression. Statistical significance was determined using paired Student's $t$-test.

## RESULTS

The neurons included in this report all responded in a manner consistent with previous characterizations of EH neurons during head-restrained eye and head movements (Chen-Huang and McCrea 1999; Cullen at al. 1993; Gdowski and McCrea 1999, 2000; Gdowski et al. 2001; McCrea et al. 1996; McFarland and Fuchs 1992; Scudder and Fuchs 1992). Specifically, neurons were modulated in response to head velocity during pWBRc and to eye velocity in the same direction during smooth-pursuit eye movements (see following text). The majority of EH neurons in our sample were classified as type I EH neurons ($n$ = 27) because they were sensitive to ipsilateral head rotations and eye movement during pWBRc and smooth pursuit. The remaining neurons ($n$ = 15) were classified as type II EH neurons because they had oppositely directed eye and head movement sensitivities during these head-restrained paradigms.

### *Head-restrained characterization*

EYE SENSITIVITY DURING FIXATION AND SINUSOIDAL SMOOTH PURSUIT. Neuronal responses of EH neurons were first quantified for a standard series of head-restrained paradigms. Figure 1*A* shows an example type I EH neuron during saccades and ocular fixation. This neuron's firing rate increased for ipsilaterally directed eye positions during intra-saccadic periods of fixation. For each cell, the relationship between mean eye position and neuronal firing rate was described using a regression analysis (Fig. 1*A*, *inset*). The eye-position sensitivity (slope = $k_x$) of our example neuron was 1.68 (spikes/s)/° and the resting discharge rate ($y$ intercept = $\text{bias}_x$) was 68 spikes/s. Prior studies have shown that this relationship is only linear over a limited range of eye positions for some EH neurons, typically spanning <25° (McFarland and Fuchs 1992). For such neurons, the analysis included only eye positions within this linear range.

Table 1 provides the average (mean ± SD) $\text{bias}_x$ and $k_x$ for our sample of type I and II EH neurons. Recall that type I EH neurons are responsive to ipsilaterally directed eye movements and head movements during pWBRc and that type II neurons are responsive to eye and head movements in the opposite direction during these paradigms. Therefore to calculate the combined population coefficient averages for eye position, the values estimated for type II neurons were first multiplied by −1 and then averaged with the type I values. A comparable procedure was used for the calculation of average eye and head movement sensitivities across type I and II EH neurons for each of the behavioral tasks in this study.

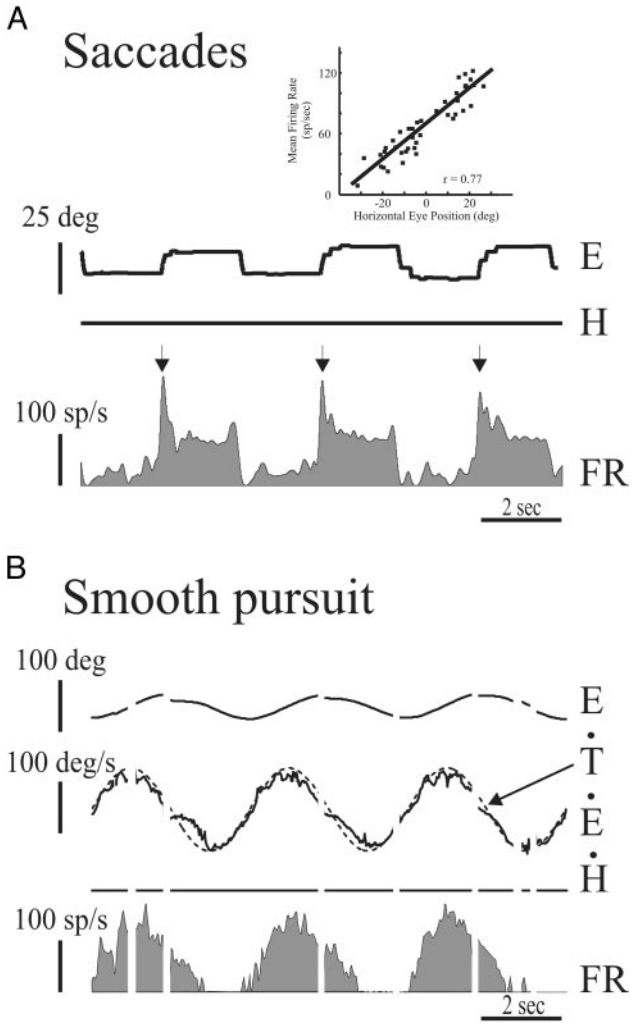


FIG. 1. Activity of an example eye-head (EH) neuron, *unit c130_1*, during the head-restrained condition. *A*: the neuron increased its discharge for ipsilaterally directed eye movements and burst for ipsilaterally directed saccades (↓). *Inset*: mean neuronal firing rate was well correlated with horizontal eye position during periods of steady fixation. *B*: the example neuron was typical in that it also increased its discharge during smooth pursuit (0.5 Hz, 40°/s peak velocity), this neuron preferred ipsilaterally directed eye movement. Traces directed upward are in the ipsilateral direction. E, eye position; H, head position; Ė, eye-in-head velocity; Ḣ, head-in-space velocity; Ṫ, target velocity; FR, firing rate.

To quantify each neuron's response during sinusoidal smooth pursuit, the following model was used: $\text{FR}(t) = \text{bias}_{sp} + k_{sp} * \text{eye position}(t) + r_{sp} * \text{eye velocity}(t)$ (pursuit model), where FR is the firing rate, $k_{sp}$ is the eye-position sensitivity, $r_{sp}$ is the eye-velocity sensitivity, and $\text{bias}_{sp}$ is the bias discharge. Overall, this model provided a good description of the discharge activity of EH neurons during smooth pursuit (mean sample VAF = 0.40 ± 0.05). For our example neuron, the estimated $\text{bias}_{sp}$ was 65 spikes/s, the $k_{sp}$ was 1.1 (spikes/s)/°, and the $r_{sp}$ was 1.13 (spikes/s)/(°/s) during pursuit of a target with a peak velocity of 40°/s (Fig. 1*B*). The average $\text{bias}_{sp}$, $k_{sp}$, and $r_{sp}$ for type I and type II neurons are listed in Table 1. For both type I and II, the mean $k_{sp}$ was significantly smaller than the $k_x$ estimated for the same neurons during fixation ($P < 0.05$). Mean phase lag with respect to eye velocity was similar for both types of neurons: 56.7 ± 20.6 and 42.8 ± 24.7°, type I and II respectively and combined mean =

TABLE 1. *Mean coefficient estimates during fixation, sinusoidal smooth pursuit, pWBRd, and pWBRc*

| | Bias, spikes/s | Eye Position (*k*) | Eye Velocity (*r*) | Head Velocity (*g*) | Head Acceleration (*a*) | Phase, ° |
|---|---|---|---|---|---|---|
| Fixation | | | | | | |
| Type I | 45 ± 38 | 1.9 ± 2.2 | — | — | — | — |
| Type II | 64 ± 40 | 0.9 ± 1.3 | — | — | — | — |
| Combined | 52 ± 39 | 1.5 ± 1.9 | — | — | — | — |
| Smooth pursuit | | | | | | |
| Type I | | | | | | |
| 40 °/s | 68 ± 40 | 1.2 ± 1.1 | 0.7 ± 0.7 | — | — | — |
| 80 °/s | 72 ± 40 | 1.0 ± 1.1 | 0.6 ± 0.5 | — | — | — |
| Type II | | | | | | |
| 40 °/s | 78 ± 40 | 0.6 ± 0.8 | 0.8 ± 1.0 | — | — | — |
| 80 °/s | 72 ± 42 | 0.8 ± 1.0 | 0.6 ± 0.8 | — | — | — |
| Combined | | | | | | |
| 40 °/s | 71 ± 40 | 1.0 ± 1.1 | 0.7 ± 0.8 | — | — | — |
| 80 °/s | 72 ± 40 | 0.9 ± 1.1 | 0.6 ± 0.6 | — | — | — |
| pWBRc | | | | | | |
| Type I | | | | | | |
| 40 °/s | 60 ± 25 | 1.0 ± 1.0 | — | 0.7 ± 0.5 | −0.04 ± 0.11 | 1.8 ± 6.2 |
| 80 °/s | 74 ± 29 | 0.9 ± 1.0 | — | 0.7 ± 0.4 | −0.06 ± 0.14 | 5.6 ± 9.9 |
| Type II | | | | | | |
| 40 °/s | 72 ± 35 | 1.0 ± 1.7 | — | 0.7 ± 0.4 | 0.01 ± 0.04 | 2.3 ± 5.1 |
| 80 °/s | 73 ± 26 | 0.9 ± 1.0 | — | 0.6 ± 0.3 | 0.03 ± 0.03 | 3.1 ± 4.9 |
| Combined | | | | | | |
| 40 °/s | 64 ± 29 | 1.0 ± 1.3 | — | 0.7 ± 0.4 | −0.02 ± 0.09 | 2.0 ± 5.8 |
| 80 °/s | 74 ± 27 | 1.0 ± 1.0 | — | 0.7 ± 0.3 | −0.03 ± 0.12 | 5.0 ± 8.8 |
| pWBRd | | | | | | |
| Type I | | | | | | |
| 40 °/s | 59 ± 43 | 0.9 ± 1.1 | — | 0.4 ± 0.4* | −0.01 ± 0.04 | 6.2 ± 16.9 |
| 80 °/s | 63 ± 45 | 1.0 ± 1.1 | — | 0.0 ± 0.5* | 0.00 ± 0.04 | 5.3 ± 11.2 |
| Type II | | | | | | |
| 40 °/s | 71 ± 34 | 0.8 ± 1.1 | — | 0.6 ± 0.3* | −0.01 ± 0.03 | 3.4 ± 9.6 |
| 80 °/s | 59 ± 22 | 1.0 ± 0.9 | — | 0.4 ± 0.3* | 0.02 ± 0.04 | 7.7 ± 11.5 |
| Combined | | | | | | |
| 40 °/s | 63 ± 40 | 0.8 ± 1.1 | — | 0.5 ± 0.3* | −0.01 ± 0.04 | 5.0 ± 14.2 |
| 80 °/s | 62 ± 22 | 1.0 ± 1.0 | — | 0.1 ± 0.5* | 0.01 ± 0.04 | 6.1 ± 11.1 |

Values are means ± SD. *, a significant difference as compared to pWBRc of $P < 0.05$. pWBRc, passive whole-body rotation where the monkey cancels its VOR; pWBRd, pWBR in the dark.

52.7 ± 22.2°. Overall, our results are consistent with those of previous studies in that neuronal eye-position sensitivities were significantly larger during fixation than during pursuit and EH neuron firing rate consistently lagged eye velocity during smooth pursuit (Cullen et al. 1993; Lisberger et al. 1994a; McFarland and Fuchs 1992).

HEAD-SENSITIVITY PASSIVE WHOLE-BODY ROTATION. The head-velocity sensitivity of each neuron was quantified during two passive whole-body rotation paradigms using the following model: FR($t$) = bias + $k$ * eye position($t$) + $g$ * head velocity($t$) + $a$ * head acceleration($t$) (pWBR model).

First we determined each neuron's bias discharge ($\text{bias}_{\text{pWBRc}}$), sensitivity to eye position ($k_{\text{pWBRc}}$), sensitivity to head velocity ($g_{\text{pWBRc}}$), and sensitivity to head acceleration ($a_{\text{pWBRc}}$) during compensatory eye movements made during WBRc. This allowed us to quantify the neuron's modulation with respect to head rotation in the absence of eye motion. The model fit for our example neuron is shown in Fig. 2*A* for pWBRc at 40°/s peak velocity (thick solid trace, pWBRc estimate; sample mean VAF = 0.37 ± 0.23). The example neuron had a $\text{bias}_{\text{pWBRc}}$ of 74 spikes/s, a $k_{\text{pWBRc}}$ of 2.2 (spikes/s)/°, a $g_{\text{pWBRc}}$ of 0.24 (spikes/s)/(°/s), and an $a_{\text{pWBRc}}$ of 0.08 (spikes/s)/(°/s$^2$) during this paradigm. Table 1 provides the mean values of coefficients estimated for the entire population of type I and II neurons. To determine if the neuronal responses to head velocity were linear, responses elicited passive whole-body rotations of 40 and 80°/s peak velocity were analyzed separately. We found that the estimated coefficients were comparable in the two conditions for both type I and II EH neurons, verifying that EH neurons respond linearly over this range (Table 1). The average phase lead of our sample EH neurons was 2.0 ± 5.8 and 5.0 ± 8.8° for 40 and 80°/s peak velocity rotations, respectively. This phase lead is comparable to that reported in previous studies that have characterized these neurons during pWBRc (Cullen at al. 1993; McFarland and Fuchs 1992; Scudder and Fuchs 1992).

Second, the pWBR model was used to quantify neuronal responses during pWBRd, in which a bias ($\text{bias}_{\text{pWBRd}}$), eye-position sensitivity ($k_{\text{pWBRd}}$), head-velocity sensitivity ($g_{\text{pWBRd}}$), and head-acceleration sensitivity ($a_{\text{pWBRd}}$) were estimated for each neuron. Note that during pWBRd, eye and head velocities are not independent—they are equal in amplitude and opposite in direction. Accordingly these terms are redundant, and as a result, it is not possible to estimate them separately.

The example neuron had a $\text{bias}_{\text{pWBRd}}$ of 72 spikes/s, a $k_{\text{pWBRd}}$ of 1.97 (spikes/s)/°, a $g_{\text{pWBRd}}$ of −0.47 (spikes/s)/(°/s), and an $a_{\text{pWBRd}}$ of 0.06 (spikes/s)/(°/s$^2$) (Fig. 2*B*, pWBRd estimate; sample mean VAF = 0.33 ± 0.25). The mean parameter values estimated for our sample of neurons are listed in Table 1. All of the neurons in the population had larger head-velocity sensitivities during pWBRc as compared with pWBRd ($P < 0.05$), and for eight type I and five type II

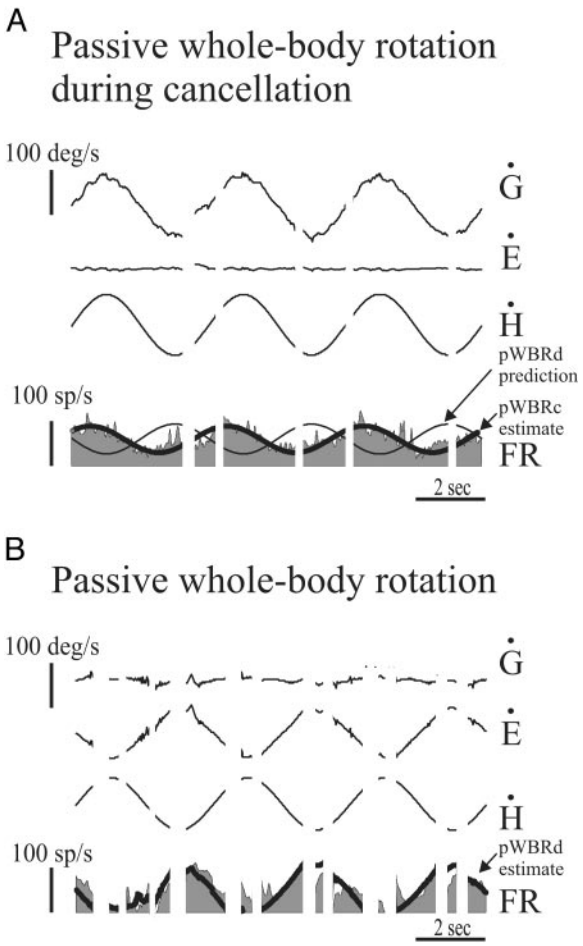


FIG. 2. Passive whole-body rotation was used to characterize each neuron's response to head movements. *A*: the example neuron, *unit c130_1*, responded to ipsilaterally directed head movement during passive whole-body rotation while the monkey cancelled its vestibuloocular reflec (VOR; pWBRc) by fixating a target that moved with the table (0.5 Hz, 40°/s peak velocity). The fit of a model based on the bias discharge, the eye-position sensitivity, and the head-velocity sensitivity is superimposed on the firing rate (pWBRc estimate, thick trace). *B*: during passive whole-body rotation in the dark (pWBRd) the example neuron responded to head movement in the contralateral direction (pWBRd estimate; thick trace). EH neurons responded with either less modulation or to head movement in the opposite direction to pWBRc. As a consequence, the discharge activity during pWBRd was a poor predictor of the activity during pWBRc (*A*; compare pWBRd prediction and pWBRc estimate, thin and thick traces, respectively). Ġ, gaze velocity (= $\dot{E}$ + $\dot{H}$).

neurons, the sensitivities were in the opposite directions during the two paradigms. Indeed, our example type I neuron's responses increased for ipsilaterally directed head rotations during pWBRc and increased for contralaterally directed head rotations during pWBRd. Accordingly, a model based on the neuron's response during pWBRd (pWBRd model) provided a strikingly poor prediction of neuronal discharge during pWBRc (Fig. 2*A*, compare pWBRd prediction with pWBRc estimate). However, the bias and eye-position sensitivities ($k$) estimated during pWBRc, pWBRd, and sinusoidal smooth pursuit were comparable ($P > 0.05$).

### *Can a linear summation of pursuit and pWBRc sensitivities predict pWBRd responses?*

Prior studies have shown that the eye- and head-velocity-related signals generated by Purkinje cells in the floccular lobe are correlated with smooth-pursuit eye movements and with head movements during pWBRc (Lisberger and Fuchs 1978; Miles et al. 1980; Stone and Lisberger 1990a). Furthermore, because these eye- and head-velocity sensitivities are nearly identical, it has been argued that these neurons encode the velocity of the axis of gaze relative to space (i.e., eye velocity during smooth pursuit and head velocity during pWBRc). Indeed, these neurons are not modulated during vestibular stimulation when gaze is stable (i.e., pWBRd) as can be predicted by summing their sensitivities to eye and head velocity during smooth pursuit and pWBRc, respectively. Similarly, the eye and head sensitivities of EH neurons are in the same direction. However, unlike gaze velocity Purkinje neurons, the eye- and head-velocity sensitivities of EH neurons are usually unequal with, on average, the eye favoring head by a ratio of 1.2:1. This result is in agreement with prior studies of EH neurons (Cullen at al. 1993; Lisberger et al. 1994a,b; McFarland and Fuchs 1992; Scudder and Fuchs 1992).

Several prior studies (Cullen at al. 1993; McFarland and Fuchs 1992; Scudder and Fuchs 1992) have investigated whether the responses of EH neurons during pWBRd can also be predicted by adding a neuron's eye- and head-velocity sensitivities during smooth pursuit and pWBRc, respectively. We carried out a comparable analysis for our sample of EH cells in which the following model was used to predict neuronal activity during pWBRd: $\mathrm{FR}(t) = \mathrm{bias}_{sp} + k_{sp} * \text{eye position}(t) + r_{sp} * \text{eye velocity}(t) + g_{pWBRc} * \text{head velocity}(t) + a_{pWBRc} * \text{head acceleration}(t)$ (pWBRd prediction), where $k_{sp}$, $r_{sp}$, and $\mathrm{bias}_{sp}$ are the eye-position sensitivity, eye-velocity sensitivity, and bias discharge that were estimated during sinusoidal pursuit (peak velocity of 40°/s), respectively, and $g_{pWBRc}$ is the head-velocity sensitivity estimated during pWBRc (peak table of 40°/s). Recall from the preceding text that the bias estimated during smooth pursuit ($\mathrm{bias}_{sp}$) and pWBRc ($\mathrm{bias}_{pWBRc}$) were comparable. Each neuron's response modulation during pWBRd is compared with that predicted by summing eye- and head-velocity sensitivities estimated during smooth pursuit and pWBRc, respectively (Fig. 3*A*). Across neurons, predictions based on summing coefficients were well correlated with coefficients estimated during pWBRd ($R^2 = 0.64$). This finding is consistent with the results of previous characterizations of EH neurons (Cullen et al. 1993; McFarland and Fuchs 1992; Scudder and Fuchs 1992). However, as noted by Scudder and Fuchs (1992) because two large signals (of opposite signs) were added to produce a smaller one, measurement errors become more significant. Thus we also compared on a neuron-by-neuron basis the difference between head-velocity sensitivities estimated during pWBRc and pWBRd to the eye-velocity sensitivity estimated during sinusoidal pursuit and found that this relationship was even more robust ($R^2 = 0.88$) and that the slope was 1.0 (Fig. 3*B*). A comparable finding was obtained when the eye/head-velocity sensitivities estimated for pursuit, pWBRd, and pWBRc at peak velocities of 80°/s were compared (data not shown). Moreover, type I and II EH neurons behaved similarly in this analysis, and in fact, the only notable difference between the two neuron subclasses during the head-restrained characterizations was that type II neurons had on average a significantly smaller eye-position sensitivity during fixation ($P < 0.05$, unpaired $t$-test). Because they encode similar signals during

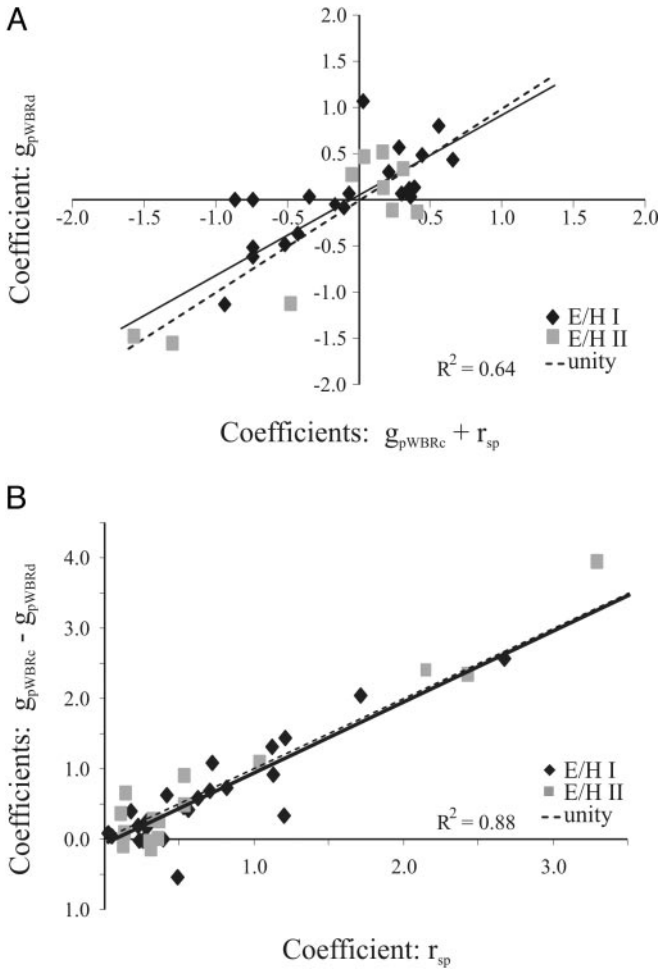


FIG. 3. Summary of eye- and head-movement sensitivities of EH neurons. *A*: when the eye- and head-velocity sensitivities estimated during head-restrained sinusoidal pursuit ($r_{sp}$) and during pWBRc ($g_{pWBRc}$), respectively, were summed, they provided an adequate prediction of the neural responses during pWBRd ($g_{pWBRd}$). *B*: EH neurons received from the floccular lobe eye and head information with similar gains. Note that the head-velocity sensitivity is the difference between that estimated during pWBRd and pWBRc. —, the best-fit regression; - - -, unity (slope = 1).

each head-restrained behavioral task, we consider type I and II EH neurons collectively in the following text.

### *Role of error terms during sinusoidal smooth pursuit*

Prior studies have shown that Purkinje cells of the cerebellar flocculus and ventral paraflocculus can encode relatively small but significant retinal slip signals (Hirata and Highstein 2001; Suh et al. 2000). Thus we tested whether EH neurons might also encode these retinal error signals by first using the following model to describe neuronal activity during sinusoidal smooth pursuit: $FR(t) = bias_{err1} + k_{err1} * \text{eye position}(t) + r_{err1} * \text{eye velocity}(t) + c_{err1} * \text{eye position error}(t\text{-lat}) + d_{err1} * \text{eye velocity error}(t\text{-lat})$ (pursuit error model 1), where FR is the firing rate, $bias_{err1}$ is the bias discharge, $k_{err1}$ is the eye-position sensitivity, $r_{err1}$ is the eye-velocity sensitivity, $c_{err1}$ is the eye-position-error sensitivity, and $d_{err1}$ is the eye-velocity-error sensitivity. Eye-acceleration and eye-acceleration-error terms were not included because these terms would be redundant with the position terms during sinusoidal tracking.

Eye-position error was calculated as the difference between target position and eye position at a specified latency (lat). Likewise, eye-velocity error was calculated as the difference between target velocity and eye velocity at the same latency. A latency of 100 ms was initially chosen to approximate the delay of visual input to these neurons (Stone and Lisberger 1990b; Suh et al. 2000). Our example neuron was typical in that during pursuit of a target with a peak velocity of 80°/s, the fit of pursuit error model 1 (Fig. 4*A*, thick trace, *bottom*) was comparable to the fit of the pursuit model (Fig. 4*A*, thick trace, *middle bottom*; VAF = 0.79 vs. 0.78, respectively). Indeed, when the goodness of fit of the models was compared on a neuron-by-neuron basis, the resulting regression slope was 0.95 (not different from 1, $P > 0.05$; Fig. 4*B*). For the population of neurons ($n = 42$), the addition of error terms at latencies of 0, 50, 75, or 100 ms only slightly improved our ability to fit the discharge of EH neurons during sinusoidal pursuit at either 40 or 80°/s (Fig. 4*C*, compare across solid columns and gray-shaded columns). For both type I and II neurons, eye-position and -velocity-error terms estimated at both velocities and across all latencies were quite small, but were nevertheless significantly different from zero (see Table 2; $P < 0.05$).

It could be argued that an individual EH neuron receives information from the Purkinje cells at a latency that was not necessarily one of the four tested. To address this possibility, the error model was estimated with latencies ranging from 0 to 130 ms during 80°/s pursuit. The model was optimized for each increment of 1 ms (i.e., a total of 130 optimizations) over this interval. For each neuron, the VAF of the model fit was comparable at all latencies. The results of this analysis for the sample of neurons ($n = 42$) are summarized in Fig. 4*D*. Based on this analysis we conclude that retinal eye-position-error or -velocity-error inputs had little influence on EH neuron responses during sinusoidal smooth pursuit.

### *Role of error term in step-ramp smooth pursuit*

It has been shown in behavioral experiments that subjects make anticipatory or predictive eye movements when tracking repetitive target trajectories such as sinusoids (Barnes and Asselman 1991; Barnes and Grealy 1992; Barnes et al. 1995, 1997; Collins and Barnes 1999). To minimize the influences of such predictive eye movements a constant-velocity step-ramp paradigm was utilized (Rashbass 1961). This type of stimuli has two advantages as compared with sinusoidal target trajectories. First, the use of step-ramp target trajectories enabled a more comprehensive characterization of the signals carried by EH neurons because eye position and acceleration do not co-vary during this paradigm as they do during sinusoidal pursuit. Second, the image slip occurring in the first 100 ms of the paradigm was much larger than that that occurred during the tracking of sinusoidal target motion. For example, retinal slip velocities were on average 40–50 versus 2–3° for 80°/s step ramps and sinusoidal target, respectively. Figure 5*A* illustrates three example trials of step-ramp pursuit for our example neuron. Note that the step component of the stimulus has been removed to simplify the presentation. The data set analyzed comprised the time period spanning from pursuit onset to 150 ms into the pursuit movement, which encompassed the acceleration phase and the beginning of the steady-state phase of

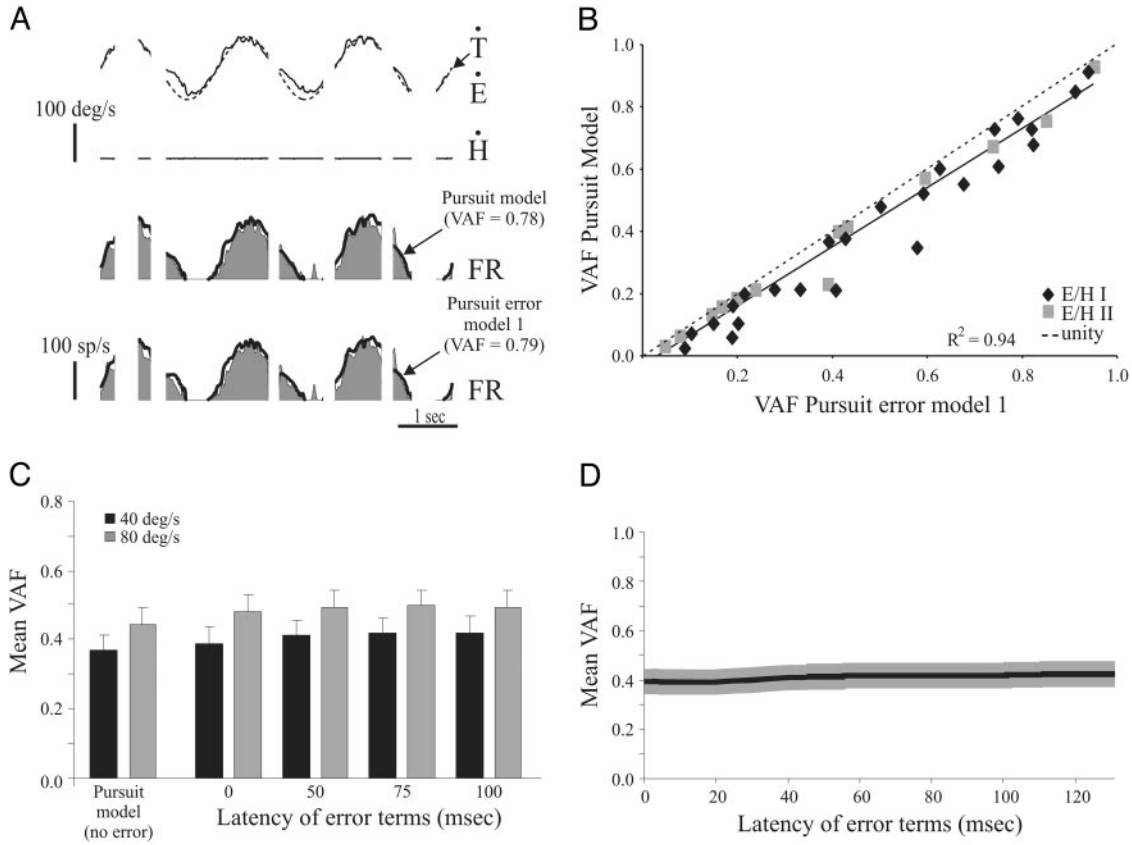


FIG. 4. EH neurons receive significant yet small inputs related to eye-position error or -velocity error during sinusoidal smooth pursuit of a sinusoidally moving target. *A*: the goodness of fit of a model that contained a bias term, an eye-position sensitivity term, and an eye-velocity term (pursuit model, *middle bottom*, thick trace) was only slightly improved when eye-position and -velocity-error terms (latency of 100 ms) was added (pursuit error model 1, *bottom*, thick trace). *B*: the variances-accounted-for (VAFs) obtained for pursuit model and pursuit error model 1 during sinusoidal pursuit were comparable for each neuron. *C*: the VAFs of the 2 models were comparable for both velocities of pursuit at the 4 different error latencies (compare solid columns for 40°/s and gray-shaded columns for 80°/s). *D*: to address whether the error latency was not 1 of the 4 previously tested, the latency was systematically shifted from 0 to 130 ms. The mean VAF did not change for the population of neurons. Error bars show SE. $\dot{T}$, target velocity; $\dot{E}_{error}$: ($= \dot{T} - \dot{E}$).

pursuit. During this time period, there was significant retinal slip and neuronal discharges were quantified using the following model: FR($t$) = $\text{bias}_{err2}$ + $k_{err2}$ * eye position($t$) + $r_{err2}$ * eye velocity($t$) + $a_{err2}$ * eye acceleration($t$) + $c_{err2}$ * eye position error($t$-lat) + $d_{err2}$* eye velocity error($t$-lat) + $e_{err2}$* eye acceleration error($t$-lat) (pursuit error model 2), where FR is the firing rate, $\text{bias}_{err2}$ is the bias discharge, $k_{err2}$ is the eye-position sensitivity, $r_{err2}$ is the eye-velocity sensitivity, $a_{err2}$ is the eye-acceleration sensitivity, $c_{err2}$ is the position-error sensitivity, $d_{err2}$ is the velocity-error sensitivity, and $e_{err2}$ is the acceleration-error sensitivity.

TABLE 2. *Eye position, velocity, and acceleration error coefficients estimated during pursuit*

| | Eye-Position Error | Eye-Velocity Error | Eye-Acceleration Error |
|---|---|---|---|
| Sinusoidal (80 °/s) | | | |
| Type I | 0.15 ± 0.23* | 0.19 ± 0.33* | — |
| Type II | 0.11 ± 0.08* | 0.21 ± 0.26* | — |
| Combined | 0.14 ± 0.20* | 0.23 ± 0.35* | — |
| Step ramp (80 °/s) | | | |
| Type I | 0.20 ± 0.33* | 0.16 ± 0.08* | 0.00 ± 0.00 |
| Type II | 0.17 ± 0.06* | 0.13 ± 0.07* | 0.00 ± 0.00 |
| Combined | 0.19 ± 0.25* | 0.15 ± 0.07* | 0.00 ± 0.00 |

Values are means ± SD; *, a significant difference of $P < 0.05$ when compared to 0.

This model construct is identical to that used by Suh et al. (2000) in their analysis of floccular lobe Purkinje cell activity during smooth pursuit. Again, a latency (lat) of 100 ms was initially chosen to approximate the delay of visual input to these neurons. For the sample of neurons tested ($n = 14$), the estimated $\text{bias}_{err2}$ (68 ± 8 spikes/s), $k_{err2}$ [1.3 ± 1.12 (spikes/s)/°], and $r_{err2}$ [1.12 ± 1.1 (spikes/s)/(°/s)] were comparable to those obtained with our original "pursuit model," which did not contain any error terms ($P > 0.05$). Indeed, as is illustrated for our example neuron, the addition of the three error terms and eye acceleration term (Fig. 5*A*, *bottom*, thick trace, VAF = 0.89) resulted in a fit comparable to the fit of the pursuit model (Fig. 5*A*, *middle bottom*, thick trace, VAF = 0.89; sample mean VAF = 0.37 ± 0.36 vs. 0.36 ± 0.24, respectively).

When considered separately, the estimated acceleration error coefficients of both type I and II neurons were not significant, and estimated position and velocity error coefficients were small but were significantly different from zero (Table 2; $P < 0.05$). Moreover, the estimated eye acceleration coefficients ($a_{err2}$) was small [−0.0002 ± 0.0002 (spikes/s)/(°/s$^2$)] and not different from zero ($P > 0.05$). Finally, the eye-position and

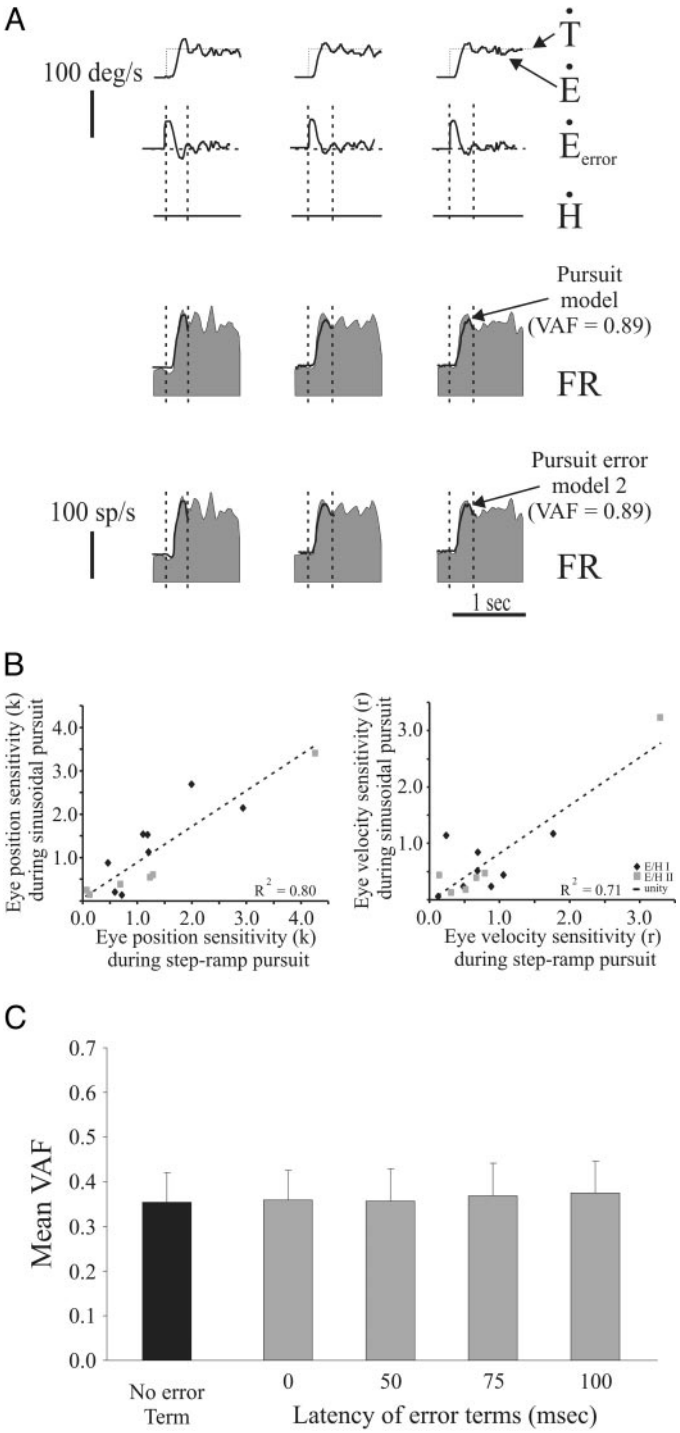


FIG. 5. EH neurons receive significant yet small inputs related to eye-position error or -velocity error during sinusoidal smooth pursuit of constant-velocity step-ramp target. *A*: as with during pursuit of a sinusoidally moving target, the VAF of pursuit error model 2 (*bottom*, thick trace) was not different from the pursuit model (*middle bottom*, thick trace). The neuronal discharges were analyzed from pursuit onset to 150 ms later (denoted by the dashed vertical lines). *B*: when compared on a neuron-by-neuron basis, the eye-position sensitivities (*left*) and eye-velocity sensitivities (*right*) were similar during sinusoidal and step-ramp pursuit. *C*: for the population of neurons, the difference in VAF was not different from when the pursuit model or pursuit error model 2 was utilized (compare solid and gray-shaded columns, respectively).

-velocity coefficients estimated during step-ramp pursuit were comparable to those estimated during sinusoidal pursuit (Fig. 5*B*, *left* and *right*, respectively).

The ability of pursuit error model 2 to fit neuronal firing rates was comparable across all latencies (0, 50, 75, or 100 ms) that were used in the model optimization (Fig. 5*C*, compare gray shaded columns). Similar results were obtained when the acceleration phase (pursuit onset to 100 ms) and the steady-state phase (100–300 ms) were analyzed separately (data not shown). Taken together, these results provide evidence that retinal error information played a negligible role in shaping EH neuron discharges.

### *EH neuron responses during combined eye-head gaze pursuit*

Once a neuron had been characterized in the head-fixed condition, the monkey's head was released from its restraint, and the same neuron was recorded during voluntary combined eye-head pursuit. Thirty-three (33) neurons remained isolated after the transition from the head-restrained to the head-unrestrained condition, and each of these neurons was analyzed during gaze shifts (see following text). Analysis of neuronal discharges during pursuit was limited to neurons recorded when the monkey generated voluntary head velocities >20°/s during combined eye-head tracking ($n = 24$). Figure 6 shows the discharge of our example neuron (Figs. 1, 2, 4, 5, and 10) during three cycles of sinusoidal pursuit (Fig. 6*A*) and during step-ramp pursuit (Fig. 6*B*). As a first step, we determined whether neuronal activity during gaze pursuit could be *predicted* using the neuron's responses during head-restrained smooth pursuit and/or passive whole-body rotation. Three specific predictions were tested. First, we attempted to predict the neuron's response based on its eye-position and -velocity sensitivities during smooth pursuit. This prediction (prediction 1) is illustrated in Fig. 6, *A* (VAF = 0.54) and *B* (VAF = 0.68), for sinusoidal and step-ramp targets, respectively. For our sample of neurons, the VAFs provided by this prediction are summarized in Fig. 7, *A* and B (□).

Second, head-movement-related terms, for which the head-velocity and -acceleration-sensitivity coefficients taken from pWBRd, were added to the model prediction (prediction 2; not shown). The simple addition of this term, however, did not significantly improve our ability to predict the firing rate during pursuit of either sinusoidal or step-ramp targets (Fig. 7, *A* and *B*, compare □ and ▨, $P > 0.05$). It was not surprising that the best prediction (prediction 3) was with a model that summed the eye-position and -velocity sensitivities estimated during smooth pursuit and head-velocity and -acceleration sensitivities taken from our analysis of the pWBRc condition: $FR(t) = bias_{sp} + k_{sp} * \text{eye position}(t) + r_{sp} * \text{eye velocity}(t) + g_{pWBRc} * \text{head velocity}(t) + a_{pWBRc} * \text{head acceleration}(t)$ (prediction 3).

This model provided a good prediction of neuronal discharge during pursuit of both sinusoidally moving (VAF = 0.77, prediction 3, Fig. 6*A*, *middle bottom*, thick trace) and step-ramp targets (VAF = 0.83, prediction 3, Fig. 6*B*, *middle bottom*, thick trace). The predictions based on this model were significantly better than those based on the previous prediction models (prediction 3, Fig. 7, *A* and *B*, ▨; $P < 0.05$).

To further quantify the responses of EH neurons during gaze pursuit, we next *estimated* the coefficients of the eye- and

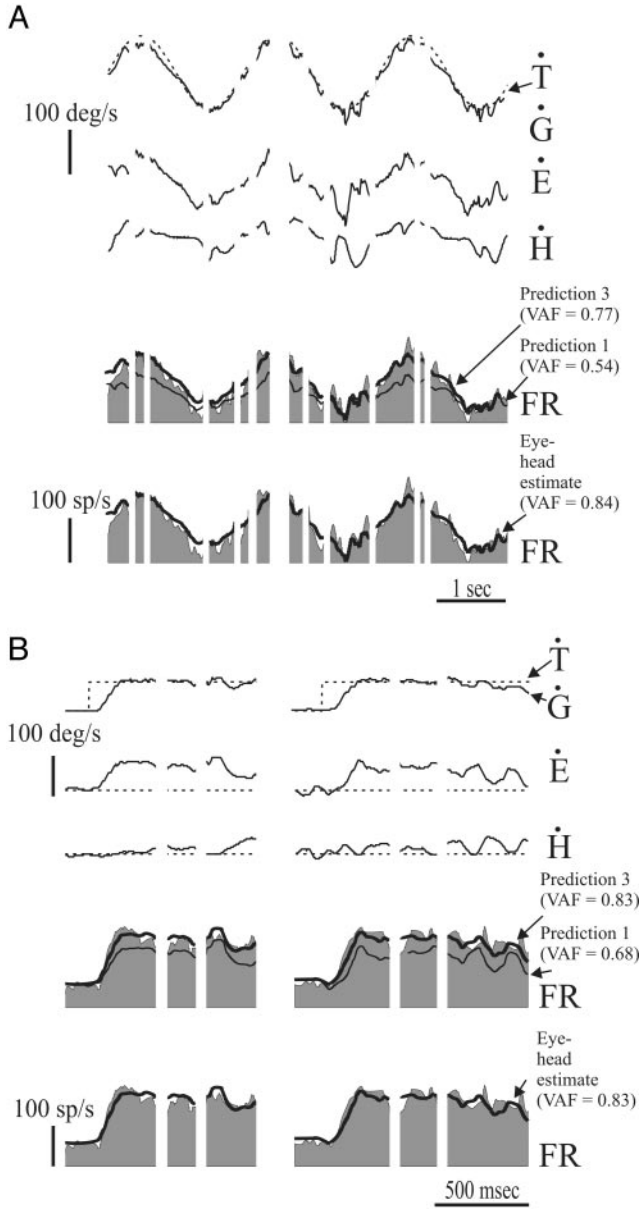


FIG. 6. Activity of EH neuron, *unit c130_1,* during combined eye-head pursuit. *A*: during pursuit of a sinusoidally moving target, a model based on neuronal responses during smooth pursuit (i.e., bias, eye position, and eye velocity) underpredicted the activity of the neuron (prediction 1, thin trace, *middle bottom;* VAF = 0.54). The best prediction model was prediction 3, which summed the eye-position and -velocity sensitivities estimated during smooth pursuit and head-velocity and -acceleration sensitivities taken from our analysis of the pWBRc condition (prediction 3, thick trace, *middle bottom;* VAF = 0.69). EH neurons responses during gaze pursuit were then estimated with a model that contained terms related to both eye and head movement (eye-head estimate, thick trace, *bottom*). *B*: a similar result was found during pursuit of step-ramp targets. Neuronal responses were underpredicted by a model based on smooth pursuit activity (prediction 1, *middle bottom*, thin trace; VAF = 0.68) and were best predicted by a model that summed the eye-position and -velocity sensitivities estimated during smooth pursuit and head-velocity and -acceleration sensitivities taken from our analysis of the pWBRc condition (prediction 3, thick trace, *middle bottom;* VAF = 0.83). As with sinusoidal pursuit, neural activity was best estimated by a model with both eye- and head-movement terms (eye-head estimate, *bottom*, thick trace; VAF = 0.83).

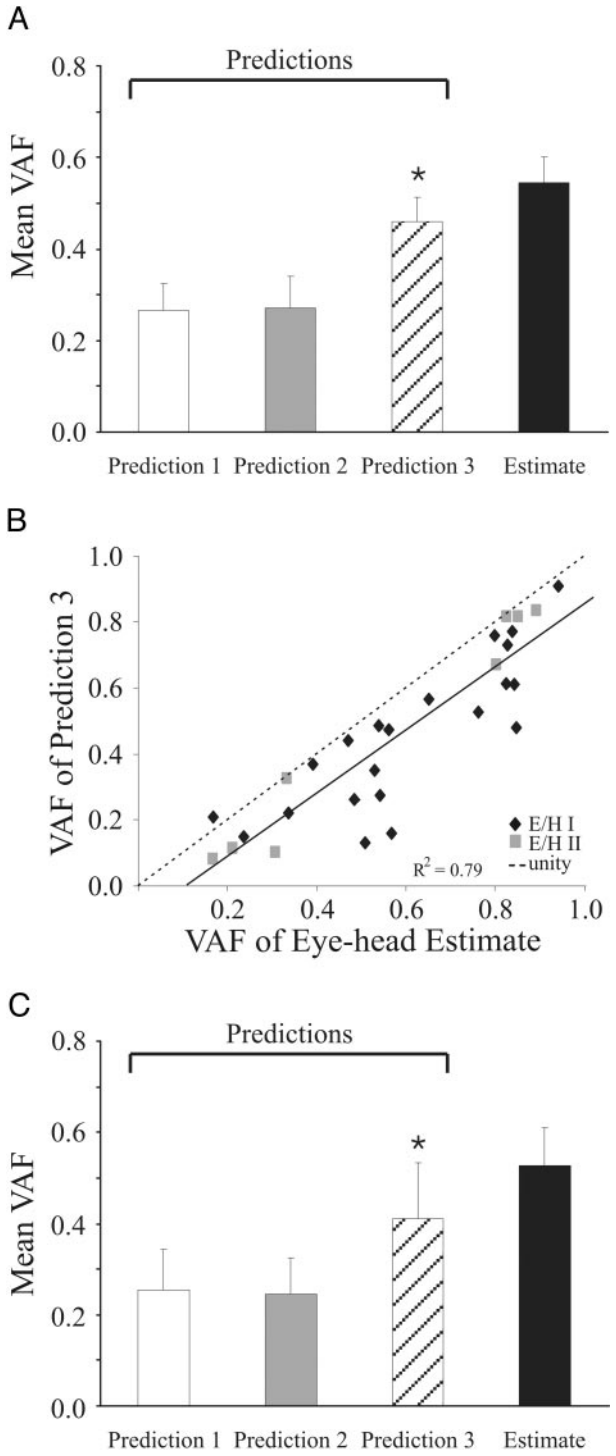


FIG. 7. Predictions of neural discharges during gaze pursuit using responses obtained from head-restrained smooth pursuit and passive whole-body rotation. *A*: a model based on neuron responses during smooth pursuit (i.e., bias, eye position, and eye velocity) provided an adequate prediction (prediction 1, □). The prediction was not improved by the addition of a head-movement-related term in which the head-velocity sensitivity coefficient was taken from pWBRd (prediction 2, ▨). The best prediction was with a model that summed the eye-position and -velocity sensitivities estimated during smooth pursuit and head-velocity and -acceleration sensitivities taken from our analysis of the pWBRc condition (prediction 3, ▨). *B*: overall, on a neuron-by-neuron basis, the VAF provided by prediction 3 was well correlated with that provided by the same model when the parameters were optimized during sinusoidal pursuit. *C*: comparable results were found during pursuit of a step-ramp target. Prediction 3 (▨) provided a significantly better prediction of the discharge activity than predictions 1 and 2 (□ and ▨, respectively).

head-related signals carried by EH neurons during gaze pursuit. A model with eye movement terms (e.g., bias, eye position, velocity, and acceleration), was first used and was found to provide a good fit to the firing rate during pursuit of sinusoidal (sample mean VAF = 0.49 ± 0.30; not shown) and step-ramp pursuit (sample mean VAF = 0.26 ± 0.28; not shown).

The addition of head velocity and head acceleration terms to the model: $FR(t) = bias_{sp} + k_{sp} *$ eye position$(t) + r_{sp} *$ eye velocity$(t) + g_{pWBRc} *$ head velocity$(t) + a_{pWBRc} *$ head acceleration$(t)$ (eye-head estimate), improved our ability to fit the responses during sinusoidal combined eye-head pursuit (sample mean VAF = 0.54 ± 0.28; Fig. 7*A*, ■). The model fit is shown in Fig. 6*A* for our example neuron (*bottom*, thick trace, eye-head estimate; VAF = 0.84). Furthermore, on a neuron-by-neuron basis, the goodness of fit (VAF) provided by prediction 3 was well correlated with, and only marginally worse than, that provided by the same model when the parameters were optimized for neuronal response during sinusoidal pursuit (slope = 0.94, not different from 1, $P > 0.05$; Fig. 7*B*).

Similar results were obtained for the analysis of combined eye-head pursuit of step-ramp targets where the eye-head estimate provided a better fit of the example neuron's discharge activity (Fig. 6*B*, bottom, thick trace, VAF = 0.83) than a model with just eye movement terms (VAF =0.68). For the subset of neurons tested during step-ramp gaze pursuit ($n = 9$), the sample mean VAF was 0.53 ± 0.25 (Fig. 7*B*, ■). Taken together, our results show that EH neurons encode head as well as eye movement related signals during combined eye-head gaze pursuit.

A comparison of the eye- and head-movement-related responses of EH neurons during head-restrained and -unrestrained pursuit paradigms was then made to determine whether they differed in these two conditions. First, to facilitate comparison, *estimated* coefficients were normalized relative to those estimated during head-restrained pursuit. We found that average estimated bias values (Fig. 8*A*), eye-position sensitivity (Fig. 8*B*), and eye-velocity sensitivity (Fig. 8*C*) were comparable across all pursuit tasks ($P > 0.05$). Second, a neuron-by-neuron comparison of the head-velocity sensitivities estimated during combined eye-head gaze pursuit and pWBRc revealed that they were comparable (slope = 0.93, not different from 1, $P > 0.05$; Fig. 9*A*). Moreover, head-velocity sensitivities of the EH neurons tested were comparable during pWBRc, sinusoidal gaze pursuit ($n = 24$, Fig. 9*B*), and step-ramp pursuit ($n = 9$, Fig. 9*C*). Thus EH neurons encode similar head-movement-related signals during these two different behavioral tasks. This is an important observation because these two head movements differ in that the head was passively rotated during pWBRc while it was voluntarily moved during gaze pursuit. In addition, head-velocity sensitivity coefficients estimated during pWBRc and gaze pursuit were significantly larger than those estimated during pWBRd (Fig. 9, *B* and *C*, compare ▨ and ■, $P < 0.05$). The implications of these findings are considered in the DISCUSSION.

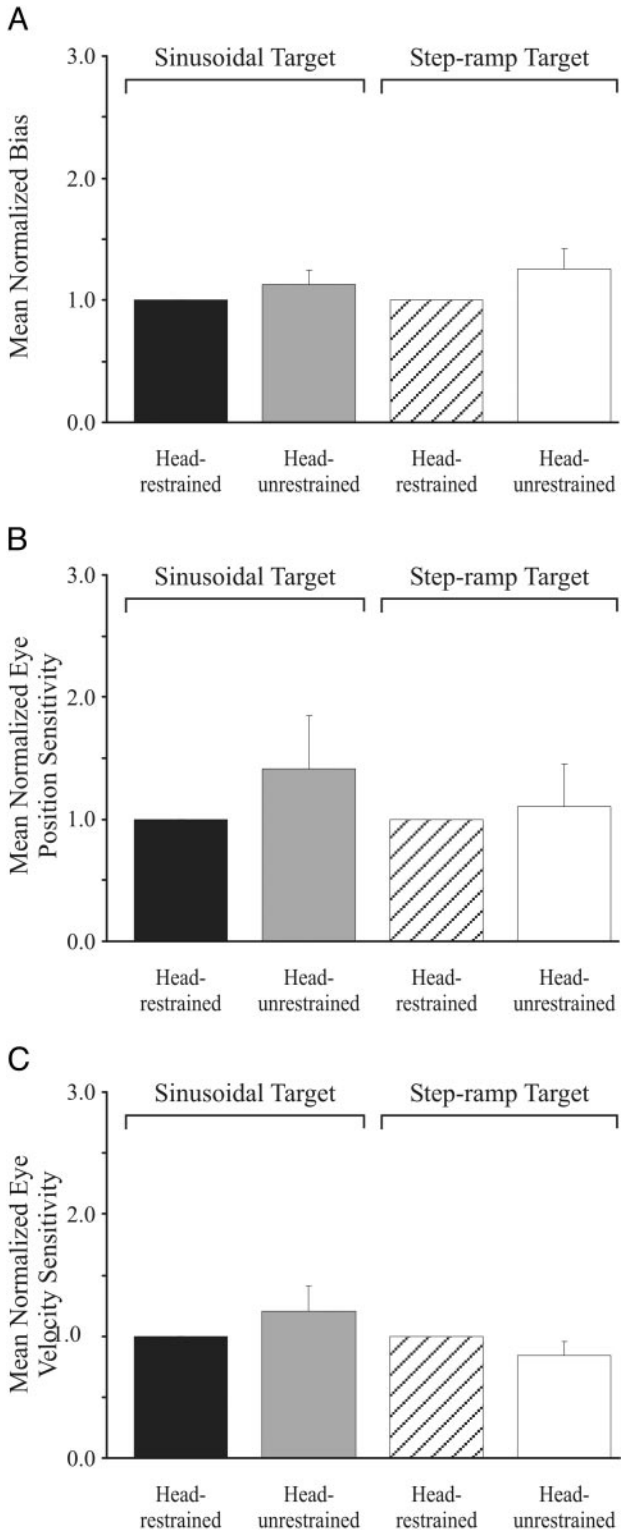


FIG. 8. Summary of bias and eye-movement sensitivities of EH neurons during pursuit. *A–C*: the bias discharge (*A*), eye-position sensitivity (*B*), and eye-velocity sensitivity (*C*) were comparable during head-restrained and -unrestrained pursuit of sinusoidal and step-ramp targets.

### *EH neuron responses during rapid gaze redirection: saccades and eye-head gaze shifts*

The responses of EH neurons were characterized during head-restrained saccades and -unrestrained gaze shifts in which the monkeys rapidly reoriented their axis of gaze in space. Nearly one-half of the EH neurons (19/42) showed a burst in discharge activity during saccades in the neuron's "on direction" during pursuit (Fig. 10*A*, *left*). The remainder were either

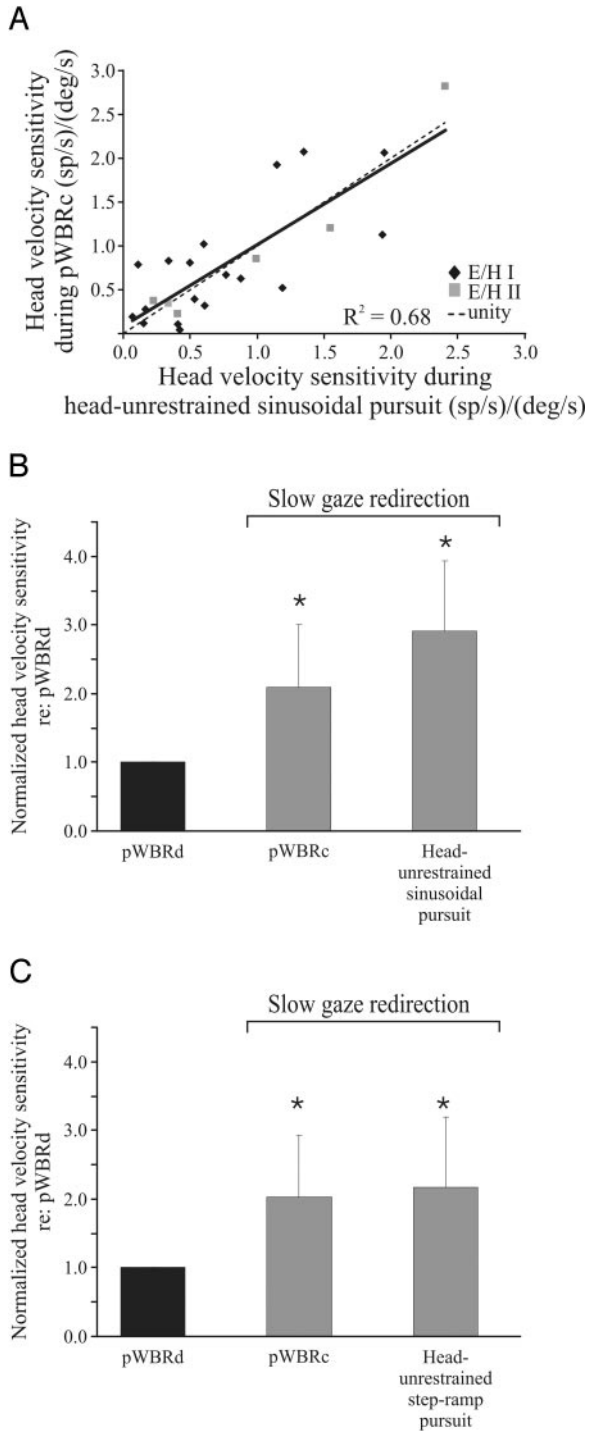


FIG. 9. Summary of head-velocity sensitivity of EH neurons. *A*: the head-velocity sensitivity of EH neurons was comparable on a neuron-by-neuron basis during pWBRc and gaze pursuit of a sinusoidally moving target. *B* and *C*: for the neurons tested, the head-velocity sensitivity was significantly greater during pWBRc and gaze pursuit of a sinusoidally moving target (*B*) and gaze pursuit of step-ramp targets (*C*) than during pWBRd (compare ▨ and ■).

unresponsive ($n = 14$, Fig. 10*A*, *right*) or paused ($n = 9$) in activity. These results are consistent with previous studies (Chen-Huang and McCrea 1999; Cullen at al. 1993; Gdowski and McCrea 1999; McFarland and Fuchs 1992; Scudder and Fuchs 1992). For the neurons that burst, the bias discharge ($\text{bias}_{\text{sac}}$), eye-position sensitivity ($k_{\text{sac}}$), and eye-velocity sensitivity ($r_{\text{sac}}$) were estimated for each neuron using the model, $\text{FR}(t) = \text{bias}_{\text{sac}} + k_{\text{sac}} * \text{eye position}(t\text{-lat}) + r_{\text{sac}} * \text{eye velocity}(t\text{-lat})$ (saccade model).

The mean $\text{bias}_{\text{sac}}$ was 106 ± 56 spikes/s, the mean $k_{\text{sac}}$ was 1.97 ± 1.10 (spikes/s)/°, and the mean $r_{\text{sac}}$ was 0.22 ± 0.17 (spikes/s)/(°/s). In addition, the mean value estimated for dynamic latency (lat) (see Cullen et al. 1996 and Sylvestre and Cullen 1999 for details) was 10 ± 9 ms, indicating that the burst lead was comparable to that which has been reported for saccadic premotor burst neurons (Cullen and Guitton 1997).

EH neurons responded in a similar manner during gaze shifts and saccades. For example, all neurons that did not burst during saccades ($n = 14$) also did not burst during gaze shifts. Similarly, all neurons that burst during on-direction saccades ($n = 19$) also burst during on-direction gaze shifts. This is illustrated in Fig. 10*B* where responses during gaze shifts of the same two neurons as in Fig. 10*A* are shown. For these latter

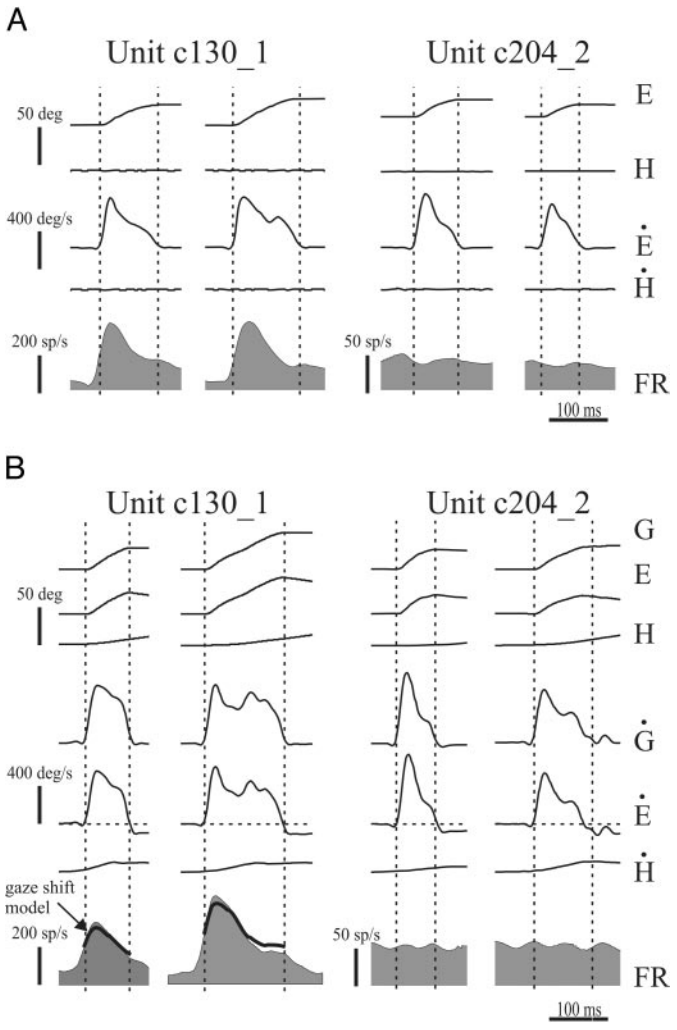


FIG. 10. Activity of example EH neurons (*units c130_1* and *c204_2*) during rapid gaze redirection. *A*: EH neuron activity during head-restrained saccades varied in that some neurons showed a burst in activity (*left*) and others did not respond (*right*) or paused in activity. *B*: the responses of EH neurons were comparable during combined eye-head gaze shifts. Neurons that burst for saccades also burst for gaze shifts (*left*). Likewise neurons that either paused or were not responsive during saccades did the same during gaze shifts (*right*). Dotted vertical lines indicate the onset and offset of gaze shifts using a ±20°/s criterion.

neurons, we found that a model based on their activity during saccades was a poor predictor of their neuronal activity during gaze shifts (sample mean VAF = 0.19 ± 0.29) suggesting that the discharge was under-modeled. A model that included a head-velocity sensitivity ($g_{gs}$), as well as a bias discharge, eye-position sensitivity, and eye-velocity sensitivity: FR($t$) = $\text{bias}_{gs}$ + $k_{gs}$ * eye position($t$-lat) + $r_{gs}$ * eye velocity($t$-lat) + $g_{gs}$ * head velocity($t$-lat) (gaze shift model), provided a much better fit on neuronal response (sample mean VAF = 0.41 ± 0.17, $P < 0.05$; Fig. 10*B*). The estimated $\text{bias}_{gs}$ and $k_{gs}$ were not significantly different from those during saccades (mean = 118 ± 56 spikes/s and 1.98 ± 1.51 (spikes/s)/°, respectively, $P > 0.05$) and the eye-velocity sensitivity was estimated to be smaller than during saccades [mean $r_{gs}$ = 0.16 ± 0.14 (spikes/s)/(°/s), $P < 0.05$]. The estimated head-velocity sensitivity of the neurons was 0.66 ± 0.63 (spikes/s)/(°/s), which was greater than that estimated for the same neurons during pWBRd ($P < 0.05$) and comparable to that estimated during pWBRc ($P > 0.05$). In contrast, the head-velocity sensitivity of EH neurons that did not burst were comparable to those estimated during pWBRd ($P > 0.05$). We also estimated the head-velocity sensitivity of EH neurons in the post gaze shift interval where gaze was stable, but the head continued to move, and found that the head velocity sensitivities of the neurons were comparable to those estimated for the same neurons during pWBRd ($P < 0.05$). These findings suggest that EH neurons encode head-motion-related information similarly during active and passive head rotations when gaze is stable.

### *Influence of neck proprioceptive inputs*

Our finding that EH neurons encoded similar head-movement-related signals during pWBRc and gaze pursuit strongly suggests that the activation of neck proprioceptors does not play a role in modulating neuronal activity during gaze pursuit. To further test this proposal, two different paradigms were used. First we passively rotated the monkey's body while holding its head earth stationary (Fig. 11*A*). The neuron shown in Fig. 11*A* was typical in that its discharge was not significantly affected by the passive neck rotations. Its activity could be well predicted by a model based on the neuron's bias and eye-position sensitivity (Fig. 11*A*, thick trace, prediction). The lack of influence was even more apparent after the firing rate was corrected for the neuron's eye-position sensitivity (Fig. 11*A*, $\text{FR}_{corr}$). The corrected response of each neuron was fit using the following model: $\text{FR}_{corr} = \text{bias}_{BUH} + n_{BUH}$ * neck velocity (BUH model), where $\text{bias}_{BUH}$ is the bias discharge, neck velocity is the velocity of the body rotation, and $n_{BUH}$ is neck-velocity sensitivity. For all the neurons tested ($n = 11$), the mean $\text{bias}_{BUH}$ of 90 ± 49 spikes/s was comparable to that measured during fixation ($P > 0.05$), and the response to passive neck proprioceptor activation was negligible [mean $n_{BUH}$ = 0.07 ± 0.17 (spikes/s)/(°/s)].

To further investigate the influence of neck proprioceptor inputs on EH neuron discharge activity, the monkey's head was passively rotated on its earth stationary body. The rotations elicited head velocities and trajectories comparable to those observed during natural head movements (Fig. 11*B*). Each neuron's discharge was characterized during this passive head-on-body rotation (PHBR) paradigm using the following model: FR = $\text{bias}_{PHBR}$ + $k_{PHBR}$ * eye position + $g_{PHBR}$ * head velocity (PHBR model) in which the bias discharge ($\text{bias}_{PHBR}$), the eye-position sensitivity ($k_{PHBR}$), and the head-velocity sensitivity ($g_{PHBR}$) were estimated during segments when gaze was stable. Overall, for the neurons tested ($n = 14$), $\text{bias}_{PHBR}$, the $k_{PHBR}$, and $g_{PHBR}$ were comparable to those values estimated during pWBRd ($P > 0.05$). Furthermore the neuron illustrated in Fig. 11*B* was typical in that when gaze was stable, a model based on the neuron's activity during pWBRd provided a good prediction of neuronal discharge (pWBRd prediction, thick trace; VAF = 0.59; sample mean VAF = 0.29 ± 0.19). Based on the results from these two approaches (BUH and PHBR paradigms), we conclude that EH neurons in the

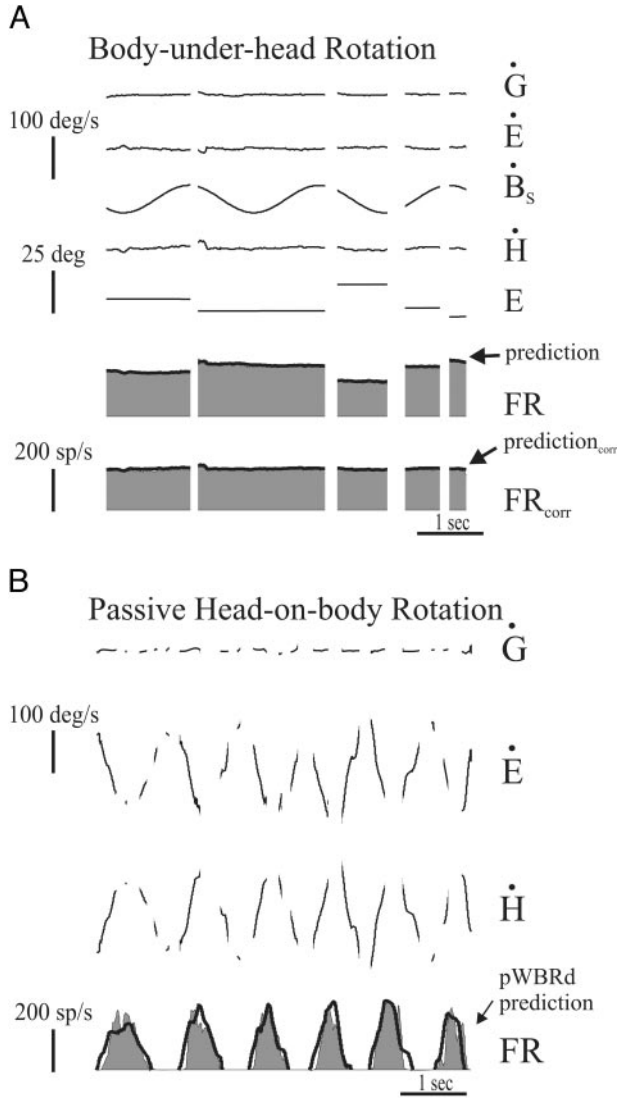


FIG. 11. Response of EH neurons to passive neck rotation. *A*: the response of example neuron (*unit cr49_1*) was typical in that it was not modulated by neck-related signals when the monkey's body was passively rotated beneath its stationary head. Neural discharges were well described by the prediction (thick trace, *middle bottom*). This is emphasized when the firing rate and prediction are corrected for the neuron's eye position sensitivity: $\text{FR}_{corr} = \text{FR} - (k_{pWBRd} * E)$ and $\text{prediction}_{corr} = \text{prediction} - (k_{pWBRd} * E)$. *B*: the response of the same neuron while the experimenter passively rotated the monkey's head relative to its earth stationary body. Neural activity was well predicted by responses during pWBRd (pWBRd prediction, thick trace). $\dot{B}$, body-in-space velocity.

alert rhesus monkey are not influenced by passive activation of neck proprioceptors.

## DISCUSSION

The neural activity of EH neurons was characterized in this study during passively induced and natural eye and head movement. Our main findings are as follows EH neurons do not encode retinal slip (i.e., eye-motion error) during the pursuit of either sinusoidally moving or step-ramp constant velocity targets, EH neurons during head-unrestrained gaze pursuit were well predicted based on their head-movement sensitivity during passive whole-body rotation in the dark and gaze-movement sensitivity during smooth pursuit, and EH neurons are not influenced by the passive activation of neck proprioceptors.

### *EH neuron activity during head-restrained pursuit*

The first goal of this study was to determine which eye-movement-based and/or error-based model best describes the discharge dynamics of EH neurons during head-restrained smooth-pursuit eye movements. The influence of error signals was tested because there are at least two possible sources from which EH neurons could potentially receive error signals: floccular lobe Purkinje cells, which have been shown to carry retinal slip information (Hirata and Highstein 2001; Suh et al. 2000), and midbrain structures such as the accessory optic system and/or the nucleus of the optic tract, which supply visual slip information to the vestibular nuclei via its projection to the inferior olive (Kato et al. 1995; Wylie and Linkenhoker 1996). We tested a range of latencies that encompassed those estimated in studies of Purkinje cells activity (Hirata and Highstein 2001: 54 ms; Stone and Lisberger 1990a: ~100 ms; Suh et al. 2000: 88 ms). Our findings are in agreement with investigations of Purkinje cell simple spike activity in which the eye-position, -velocity, and -acceleration error-related activity were significant but were so small that they essentially played no role in shaping neuronal discharges during pursuit (Hirata and Highstein 2001; Suh et al. 2000).

Purkinje cell simple spike activity has been shown to be correlated with complex spike activity at frequencies >5Hz but not at lower frequencies of 0.5 and 2 Hz during VOR adaptation (Raymond and Lisberger 1997, 1998). Thus it is possible that retinal slip would have played a more important role in modulating neuronal activity at higher frequencies of stimulation than those used in the current study. Nevertheless, we found that EH neurons are not significantly influenced by error terms during a step-ramp target pursuit task in which retinal slip is more transient. Moreover it is interesting to note that the activity of neurons within the nucleus of the optic tract and accessory optic system can be modulated by visual slip during sinusoidal pursuit at 0.5 Hz (Mustari and Fuchs 1989; Yakushin et al. 2000). Taken together, our results suggest that during pursuit, any sensory visual inputs to EH neurons have been completely transformed into an oculomotor command signal.

### *EH neurons are not influenced by passive neck proprioceptive information*

The second goal of this study was to determine whether the passive activation of neck proprioceptors influences the discharge behavior of EH neurons. Studies in squirrel monkey have suggested that EH neurons respond to changes in neck position or velocity during passive rotation of the monkey's body with its head-held stationary in space (Gdowski and McCrea 2000; Gdowski et al. 2001). In contrast, when we tested neurons with a comparable paradigm in the present study, we found no influence of passive neck activation in rhesus monkeys (Fig. 11*A*). Gdowski and colleagues (Gdowski and McCrea 2000; Gdowski et al. 2001) also tested neurons during a paradigm in which the monkey's head was passively rotated on its earth-stationary body and found that neuronal responses to head motion were different from during passive whole-body rotation. They argued that EH neurons could mediate, in part, the cervicoocular reflex (COR), which functions to produce compensatory eye movements in response to unexpected neck motion. In contrast, we have shown here that neuronal responses to head motion were comparable during passive head-on-body and passive whole-body rotations (Fig. 11*B*). One possible explanation for the difference in results is that the COR is more robust in squirrel monkeys than it is in rhesus monkeys. Indeed, it appears that squirrel monkeys have a significant COR (gain = 0.4) (Gdowski et al. 2001), whereas vestibular intact rhesus monkeys do not (gain = 0) (Bohmer and Henn 1983; Dichgans et al. 1973; Roy and Cullen 2002). In addition, EH neurons are not the only neurons within the vestibular nucleus that show differences regarding their sensitivity to passive activation of neck proprioceptors for these two species. Other second-order neurons, namely position-vestibular-pause neurons and vestibular-only neurons appear to be influenced by passive neck activation in squirrel monkey (Gdowski and McCrea 1999, 2000; Gdowski et al. 2001; McCrea et al. 1999) but not in rhesus monkey (Roy and Cullen 2001, 2002).

### *Analysis of EH neurons during gaze pursuit*

The primary goal of this study was to determine what signals are encoded by EH neurons during combined eye-head gaze pursuit. Several lines of evidence in the current study indicate that EH neurons carry vestibular signals, in addition to eye and/or gaze related signals, during gaze pursuit. First, a prediction model based solely on each neuron's sensitivity to eye (= gaze) movement during head-restrained smooth-pursuit (i.e., bias, eye position, and eye velocity) failed to fully account for discharges during gaze pursuit (Fig. 7, *A* and *B*). Second, neuronal activity during gaze pursuit was best quantified by a model that contained both, but not equal, eye- and head-movement terms (Fig. 6, *A* and *B*). Third, the head-velocity sensitivities estimated during gaze pursuit and pWBRc—behavioral tasks in which gaze was slowly redirected—were similar (Fig. 12*A*, compare □). These two tasks differ in that the head movement is actively generated in gaze pursuit, but it is passively applied in pWBRc.

### *Vestibular inputs to EH neurons*

EH neurons are known to receive vestibular-related signals via direct inputs from the ipsilateral vestibular afferents (Broussard and Lisberger 1992; Chen-Huang and McCrea 1999; Gdowski and McCrea 1999, 2000; Scudder and Fuchs 1992) as well as polysynaptic inputs from the contralateral vestibular nerve (Broussard and Lisberger 1992). In addition,

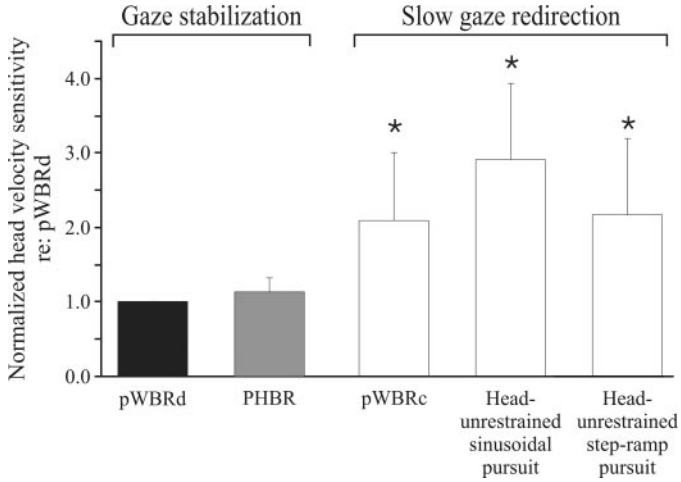


FIG. 12. Summary of EH neuron head-velocity sensitivities during gaze stabilization and redirection. EH neurons had comparable head-velocity sensitivities whenever the monkey's goal was to slowly redirect its gaze either during pWBRc and eye-head pursuit of a sinusoidally moving or step-ramp target (□). During these behavioral tasks, the head-velocity sensitivities were significantly greater that those estimated when the monkey's goal was to stabilize its gaze during pWBRd (■) and passive head-on-body rotation (PHBR, ▨).

inputs from floccular lobe Purkinje cells carry head-velocity signals during passive whole-body rotation when monkeys redirect their gaze by fixating a target that moves with the head (Belton and McCrea 2000a,b; Büttner and Waespe 1984; Lisberger and Fuchs 1978; Miles et al. 1980). For a subset of neurons, the short latency vestibular afferent input was confirmed by braking the head for a short-duration during step-ramp pursuit ($n = 5$; Fig. 13*A*) or applying high-acceleration, short-duration pulses of head motion during steady fixation ($n = 2$, Fig. 13*B*). On average, neurons responded to these perturbations with a latency of 6.35 ± 1.39 ms, which is much less than that required of a response based on visual information (~100 ms) (Carl and Gellman 1987; Cullen et al. 1991; Dubrovsky and Cullen 2002). This value is similar to, though slightly smaller than the latency of 12.9 ms reported by Lisberger et al. (1994b). The latter study differs from ours in that we have used transient head perturbations with peak head decelerations/accelerations between 2,500 and 10,000°/s$^2$ (Huterer and Cullen 2002), whereas the transient head stimulus used by Lisberger et al. (1994a) involved much smaller accelerations (600°/s$^2$). The larger head acceleration used in the present study would yield a more accurate, and shorter, estimate of latency (see discussion of Cullen et al. 1996). However, these results differ from a study in squirrel monkey in which the majority of EH neurons responded to unpredictable steps of head acceleration during pWBRd and pWBRc with a latency of 70–100 ms (Cullen et al. 1993). It is likely that the large discrepancy between the latencies observed in studies of rhesus versus squirrel monkeys reflects a species difference. As was noted in the preceding text, there is accumulating evidence that there may be some differences in the processing which is done by the vestibular nuclei of squirrel monkeys and rhesus monkeys (for example, see Gdowski and McCrea 2000; Roy and Cullen 2001).

### *Floccular inputs to EH neurons*

There is controversy over whether the signals from the floccular lobe to the EH neurons encode eye-head (gaze) motor commands or eye motor commands. On the one hand, there is considerable evidence supporting the idea that floccular inputs to the vestibular nuclei encode gaze-related information. First, a subset of Purkinje cells respond similarly to eye velocity and head velocity during head-restrained pursuit (where eye velocity = gaze velocity) and pWBRc (where head velocity = gaze velocity), respectively, suggesting that these neurons encode gaze velocity (Fukushima et al. 1999; Kahlon and Lisberger 2000; Lisberger and Fuchs 1978; Miles et al. 1980). Second, patients with cerebellar disease show similar deficits while tracking targets with only their eyes or with combined eye-head movements (Waterston et al. 1992). Third, the flocculus

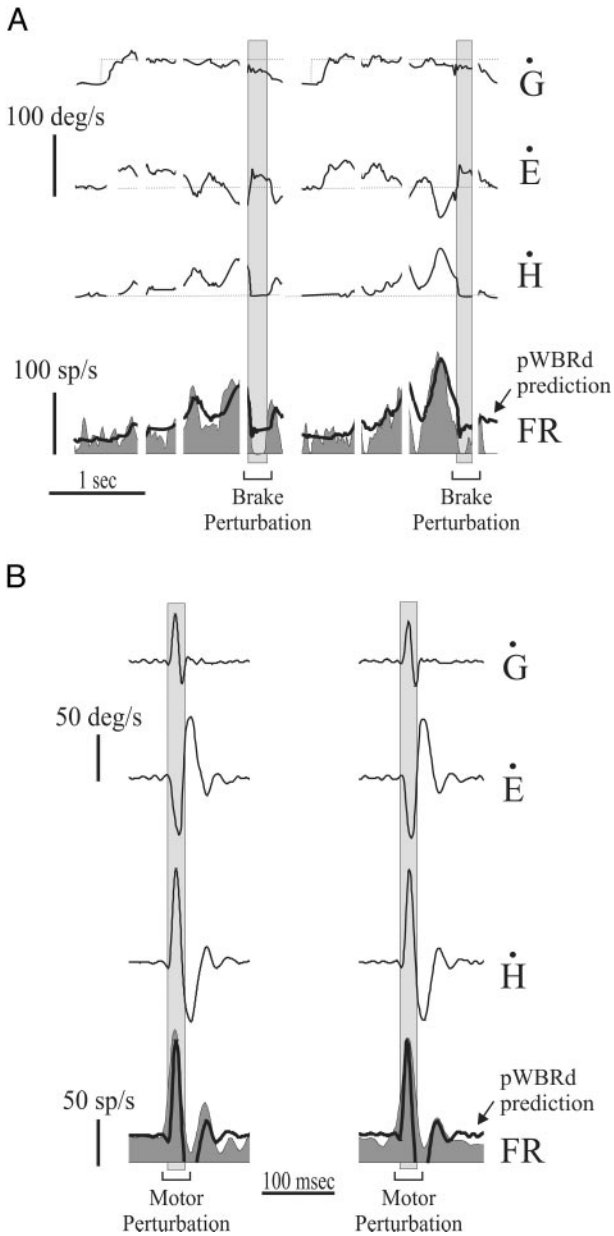


FIG. 13. EH neuron responses during head perturbations. *A* and *B*: the responses of a subset of EH neurons were recorded while braking the head for a short-duration during step-ramp pursuit (*A*) and while high-frequency and high-velocity short-duration perturbations were applied to the head during steady fixation (*B*). The neural activity could be well predicted by a model based on responses during pWBRd (pWBRd prediction, thick traces). ▨ stimulus interval of either the brake or the motor.

and ventral paraflocculus receive inputs from cortical regions involved in generating pursuit commands via the dorsolateral pontine nucleus (for review, see Keller and Heinen 1991). Neurons within the medial superior temporal sulcus (MST) and frontal eye fields (FEF) have been shown to encode retinal image and/or gaze velocity signals (Fukushima et al. 2000; Kawano et al. 1984; Komatsu and Wurtz 1988; Newsome et al. 1988; Sakata et al. 1983). Accordingly, it has been proposed that these structures provide both target velocity-in-space and gaze velocity commands to downstream structures (Fukushima et al. 2000; Newsome et al. 1988; Tanaka and Fukushima 1998).

On the other hand, studies in squirrel monkey found that eye movements were profoundly affected but that head movements remained relatively unaffected when the floccular lobe was inactivated with muscimol (Belton and McCrea 2000b). Moreover, during gaze pursuit, most squirrel monkey Purkinje cells encode eye movement signals and only a minority remain as sensitive to gaze velocity as during smooth pursuit (Belton and McCrea 2000b). The authors interpreted these results as evidence that eye and head must be controlled separately because the Purkinje cells carry signals to drive only eye movements (Belton and McCrea 2000b). However, in considering this result, it is important to note that the squirrel monkey floccular lobe does not appear to have the same composition of Purkinje cell types as does the rhesus floccular lobe. The occurrence of Purkinje cells that respond to both eye movements during head-restrained pursuit and head movement during pWBRc is rare (Belton and McCrea 2000a,b) as opposed to rhesus monkey where they are predominant (Fukushima et al. 1999; Lisberger and Fuchs 1978; Miles et al. 1980; Stone and Lisberger 1990a). Thus it seems that neurons in the floccular lobe, as well as in the vestibular nuclei may encode different information in squirrel monkey and rhesus monkey. Based on the analysis which is presented in the following text, we suggests that EH neurons carry signals related to both gaze and head motion during gaze pursuit and argue that this is consistent with predictions based on floccular lobe recordings in the rhesus monkey.

Illustrated in Fig. 14 are the structures thought to send projections to EH neurons: namely the vestibular afferents and the floccular lobe Purkinje cells. Vestibular afferents from the ipsilateral nerve are known to project to EH neurons (Broussard and Lisberger 1992; Chen-Huang and McCrea 1999; Gdowski and McCrea 1999, 2000; Scudder and Fuchs 1992). Although not directly tested, evidence suggests that the floccular lobe projects to EH neurons because during head-restrained paradigms they resemble flocculus target neurons (FTN), which do receive direct projections (Broussard and Lisberger 1992; Lisberger and Pavelko 1988; Lisberger et al. 1994a,b). An input from neck proprioceptors via the central cervical nucleus (Sato et al. 1997) has been omitted because we have determined that EH neurons, at least in the rhesus monkey, are not modulated in response to passive or voluntary activation. By the same logic, error-related inputs from the nucleus optic tract and accessory optic system are not shown.

When the monkey's goal was to stabilize its gaze by generating a VOR during passive whole-body rotation (pWBRd), the main input to the EH neurons arose from the vestibular afferents (Fig. 14*A*, $g_{aff}$). Input from the Purkinje cells should be negligible given that the sensitivities of the gaze velocity Purkinje cells in rhesus monkey to eye and head movement are nearly equal (Lisberger and Fuchs 1978; Miles et al. 1980; Stone and Lisberger 1990a). We found that on average the head-velocity sensitivity of both type I and II subpopulations of EH neurons are close to zero during pWBRd. Thus it seems unlikely that projections from EH neurons to the abducens nucleus (Scudder and Fuchs 1992) impact VOR function in this condition. This proposal is consistent with prior studies that have shown that inactivation of the flocculus has little effect on the behavioral VOR gain (Partsalis et al. 1995; Zhang et al. 1995a,b). We suggest that the contribution of EH neurons becomes significant in situations where the VOR gain must be modified such as during adaptation following spectacle-induced motor learning (Lisberger 1994; Lisberger et al. 1994a), and vestibular injury.

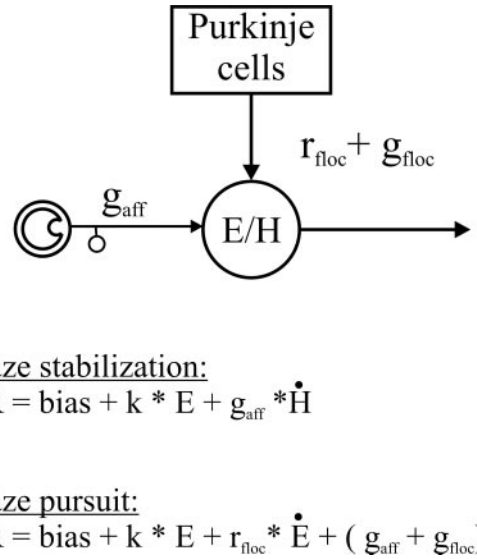


FIG. 14. Simplified schema of the structures thought to send projections to EH neurons. EH neurons are known to receive projections from the vestibular afferents and evidence suggests that the floccular lobe projects to EH neurons. Given that the sensitivities of the gaze-velocity Purkinje cells in rhesus monkey to eye and head movement are nearly equal, during gaze stabilization (i.e., VOR) EH neurons are modulated primarily from the vestibular afferent input ($g_{aff}$). In contrast, during slow gaze redirection (i.e., gaze pursuit) EH neurons receive head-movement information from the vestibular afferents ($g_{aff}$) as well as eye ($r_{floc}$)- and head ($g_{floc}$)-movement signals or gaze information from the Floccular lobe.

When the monkey's goal was to slowly redirect its gaze, inputs from the Purkinje cells were no longer negligible. For example, during head-restrained smooth pursuit, EH neurons receive eye-velocity information (where eye = $g_{floc}$) via this projection. During cancellation of the VOR, in which the monkey voluntarily redirects its gaze by fixating a target that moves with the head, EH neurons receive head velocity information from not only the majority of Purkinje cells ($g_{floc}$), but also from the vestibular afferents ($g_{aff}$). This summing of signals could explain why prior studies concluded that the eye-velocity sensitivity of EH neurons was larger than the head-velocity sensitivity during pWBRc (Cullen et al. 1993; McFarland and Fuchs 1992; Scudder and Fuchs 1992). However, when the difference between neuronal responses during pWBRd and pWBRc is calculated, the head- and eye-velocity-related sensitivities of EH neurons are comparable (Fig. 3*B*), further supporting the idea that Purkinje cell input is a gaze motor command, which reflect the summation of eye-in-head + head-in-space velocity.

To test the hypothesized schema in Fig. 14, we determined

whether the activity of EH neurons during eye-head gaze pursuit could be predicted by the linear sum of the eye-velocity sensitivity during smooth pursuit (i.e., $r_{floc}$) and the head-velocity sensitivity during pWBRc (i.e., $g_{aff} + g_{floc}$). Put another way this means that during gaze pursuit, EH neurons would receive head-movement-related inputs from the vestibular afferents (i.e., $g_{aff}$) and gaze-movement-related information from the floccular lobe (i.e., $r_{floc} + g_{floc}$). Indeed, we found that the activity could be well predicted (Fig. 7, *A* and *B*, ▨). We conclude that, during active and passive head movements, EH neurons encode eye and head movements in a manner that reflects the monkeys current gaze strategy. The discharge activity of EH neurons during the different paradigms is summarized in Fig. 15*A*. When the monkey's goal is to stabilize its gaze, EH neurons respond in a comparable manner (Fig. 15*A*, *left*, solid columns) and when the goal is to redirect gaze either slowly (blue columns) or rapidly (red columns) responses were significantly greater. As outlined in the preceding text, the

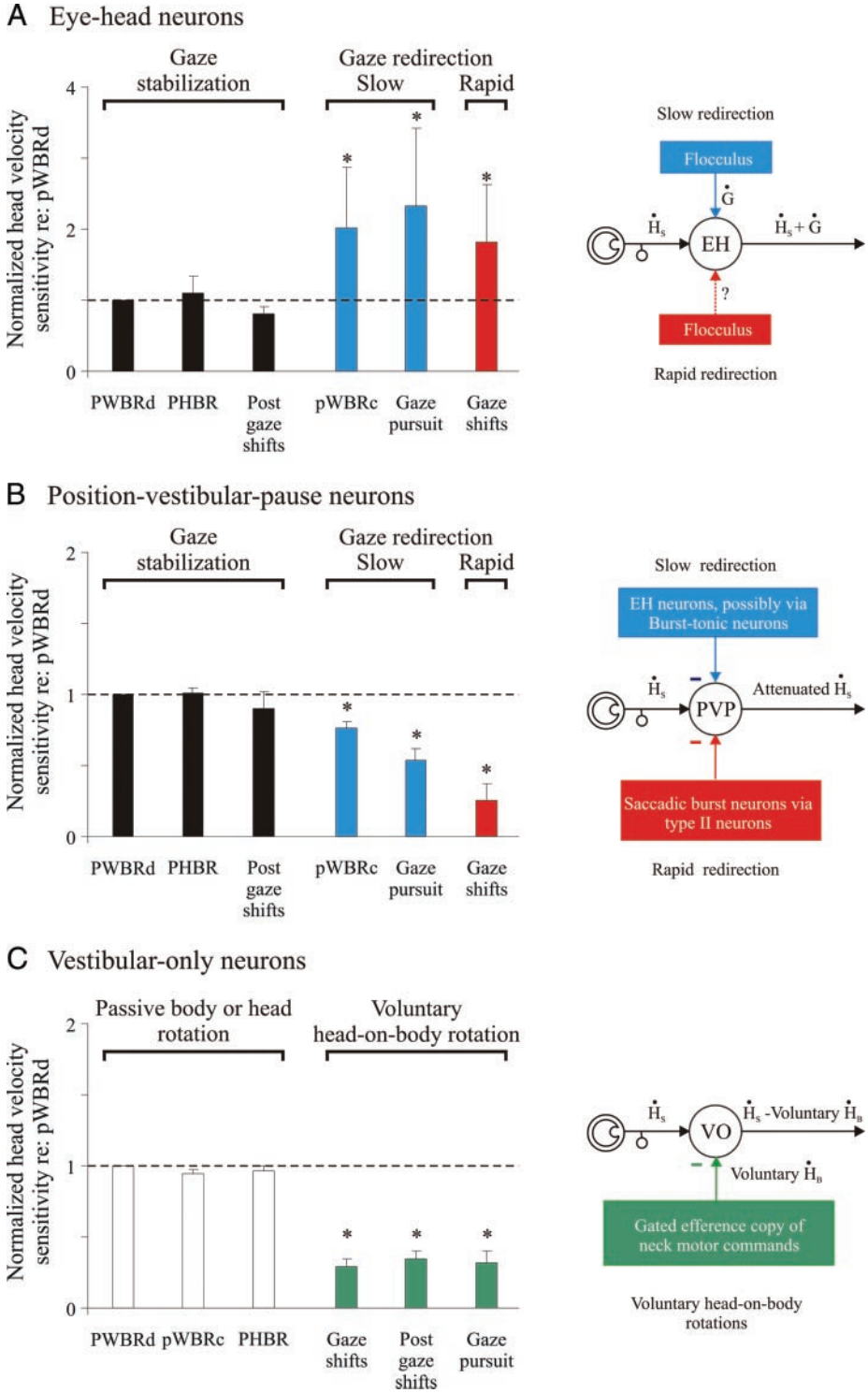


FIG. 15. A comparison of EH, position-vestibular-pause (PVP), and vestibular-only (VO) neuron head-velocity-related modulation. *A*: when the monkey's goal is to stabilize its gaze, EH neurons respond in a comparable manner (*left*, solid columns) and when the goal is to redirect gaze either slowly (blue columns) or rapidly (red columns) responses were significantly greater. We propose that the behavioral dependent modulation is mediated by a floccular lobe Purkinje cell input during both rapid and slow gaze redirection (*right*). *B*: the head-velocity-related modulation of PVP neurons is comparable whenever monkeys stabilized their gaze relative to space (*left*, solid columns) and is significantly reduced whenever monkeys redirect their gaze relative to space either slowly (blue columns) or rapidly (red column). The behavioral-dependent attenuation is thought to be mediated via premotor circuitries known to generate slow (*right;* blue box) and rapid gaze redirection (*right;* red box). *C*: the head-velocity-related modulation of VO neurons was not dependent on the gaze strategy (i.e., stabilize or redirect gaze) but rather on the source of the head motion. VO neurons faithfully encoded head velocity for all head motion that was not generated via voluntary activation of the neck musculature (*left*, open columns) and showed significant attenuation for all head motion generated by the voluntary activation of the neck musculature (green columns). The attenuation is most likely mediated either directly or indirectly by an efference copy of the neck motor command (*C*, *right*, green box). $\dot{H}$, head-in-space velocity; $\dot{H}_B$, head-on-body velocity.

behavioral-dependent modulation during slow gaze redirection is most likely mediated by a floccular lobe Purkinje cell input (Fig. 15*A*, *right*, blue box). Similarly, because a subset of Purkinje cells also burst during saccades (Lisberger and Fuchs 1978; Noda and Suzuki 1979), they could similarly play a role in shaping EH neuron responses during rapid gaze redirection (Fig. 15*A*, *right*, red box).

EH neurons are not the only neurons in the vestibular nuclei whose neural discharges are dependent on the monkeys' behavioral goals. We have previously shown that the head-velocity-related modulation encoded by position-vestibular-pause (PVP) neurons, the interneurons that mediate the VOR, is comparable whenever monkeys stabilize their gaze relative to space (Fig. 15*B*, *left*, solid columns). In contrast, their responses to head velocity are significantly reduced whenever monkeys redirect their gaze relative to space either slowly (blue columns) or rapidly (red column). This behavioral-dependent attenuation is most likely mediated via inputs from premotor circuitries known to generate slow (Fig. 15*B*, *right*, blue box) and rapid (*right*, red box) gaze redirection (for details, see Roy and Cullen 2001). Moreover, the head-velocity-related modulation of a third class of neurons, vestibular-only (VO) neurons, is also behaviorally dependent (Roy and Cullen 2002). In contrast to EH and PVP neurons, VO neuron discharge activity was not dependent on the gaze strategy (i.e., stabilize or redirect gaze) but rather on the nature of the head motion. VO neurons faithfully encoded head velocity for all head motion that was not generated via voluntary activation of the neck musculature (Fig. 15*C*, *left*, open columns) and showed significant attenuation for all head motion generated by the voluntary activation of the neck musculature (green columns). We propose that the attenuation is consistent with their proposed role in mediating the vestibulocollic reflex and is mediated either directly or indirectly by an efference copy of the neck motor command (Fig. 15*C*, *right*, green box) (for details, see Roy and Cullen 2002).

### *Functional implications*

The activity of EH neurons are thought to be essential for generating smooth-pursuit eye movements during head-restrained tracking (Cullen at al. 1993; Lisberger et al. 1994a,b; McFarland and Fuchs 1992; Scudder and Fuchs 1992). Here we provide evidence that during combined eye-head pursuit EH neurons carry gaze as well as head-velocity information. We suggest that these inputs arise from the floccular lobe and vestibular afferents, respectively. However, the exact nature of upstream signals that drive EH neurons during gaze pursuit remains to be confirmed. Because at least some EH neurons project to the abducens nucleus, it is important to note that these neurons effectively carry inappropriate head-velocity information to the extraocular motoneurons during combined eye-head pursuit. We suggest that this inappropriate input is removed at the level of the abducens nucleus by inputs from PVP neurons. During gaze pursuit, PVP neurons are active: their head-velocity-related responses are attenuated by only ~30% relative to VOR in the dark (Fig. 15*B*) (Roy and Cullen 2002). Thus we can conclude that the head-velocity-related responses of PVP neurons contribute significantly to offsetting those of the EH cells.

We thank P. A. Sylvestre, S. Sadeghi, and M. McCluskey for critically reading the manuscript and E. Moreau, W. Kucharski, J. Knowles, and A. Smith for excellent technical assistance.

This study was supported by the Canadian Institutes of Health Research.

## REFERENCES

**Anastasopoulos D and Mergner T.** Canal-neck interaction in vestibular nuclear neurons of the cats. *Exp Brain Res* 46: 269–280, 1982.

**Balaban CD, Ito M, and Watanabe E.** Demonstration of zonal projections from the cerebellar flocculus to vestibular nuclei in monkeys (*Macaca fuscata). Neurosci Lett* 27: 101–105, 1981.

**Barnes GR.** Visual-vestibular interaction in the control of head and eye movement: the role of visual feedback and predictive mechanisms. *Prog Neurobiol* 41: 435–472, 1993.

**Barnes GR and Asselman PT.** The mechanism of prediction in human smooth pursuit eye movements. *J Physiol* 439: 439–461, 1991.

**Barnes GR and Grealy MA.** Predictive mechanisms of head-eye coordination and vestibulo-ocular reflex suppression in humans. *J Vestib Res* 2: 193–212, 1992.

**Barnes GR, Goodbody S, and Collins S.** Volitional control of anticipatory ocular pursuit responses under stabilized image conditions in humans. *Exp Brain Res* 106: 301–317, 1995.

**Barnes GR, Grealy M, and Collins S.** Volitional control of anticipatory ocular smooth pursuit after viewing, but not pursuing, a moving target: evidence for a re-afferent velocity store. *Exp Brain Res* 116: 445–455, 1997.

**Belton T and McCrea RA.** Contribution of the cerebellar flocculus to gaze control during active head motion. *J Neurophysiol* 81: 3105–3109, 1999.

**Belton T and McCrea RA.** Role of the cerebellar flocculus region in cancellation of the VOR during passive whole body rotation. *J Neurophysiol* 84: 1599–1613, 2000a.

**Belton T and McCrea RA.** Role of the cerebellar flocculus region in the coordination of eye and head movements during gaze pursuit. *J Neurophysiol* 84: 1614–1626, 2000b.

**Bloedel JR and Courville J.** A review of cerebellar afferent systems. In: *Handbook of Physiology. The Nervous System. Motor Control.* Bethesda, MD: Am Physiol Soc, sect. 1, vol. II, chapt. 16, p. 735–829, 1981.

**Bohmer A and Henn V.** Horizontal and vertical vestibuloocular and cervicoocular reflexes in the monkey during high frequency roration. *Brain Res* 277: 241–258, 1983.

**Boyle R and Pompeiano O.** Responses of vestibulospinal neurons to sinusoidal rotation of the neck. *J Neurophysiol* 44: 633–649, 1981.

**Broussard DM and Lisberger SG.** Vestibular inputs to brain stem neurons that participate in motor learning in the primate vestibuloocular reflex. *J Neurophysiol* 68: 1906–1909, 1992.

**Büttner U and Waespe W.** Purkinje cell activity in the primate flocculus during optokinetic stimulation, smooth pursuit eye movements and VOR suppression. *Exp Brain Res* 55: 97–104, 1984.

**Carl JR and Gellman RS.** Human smooth pursuit: stimulus-dependent responses. *J Neurophysiol* 57: 1446–1463, 1987.

**Chen-Huang C and McCrea RA.** Effects of viewing distance on the responses of vestibular neurons to combined angular and linear vestibular stimulation. *J Neurophysiol* 81: 2538–2557, 1999.

**Collins S and Barnes GR.** Independent control of head and gaze movements during head-free pursuit in humans. *J Physiol* 515: 299–314, 1999.

**Cullen KE, Belton T, and McCrea RA.** A non-visual mechanism for voluntary cancellation of the vestibulo-ocular reflex. *Exp Brain Res* 83: 237–252, 1991.

**Cullen KE, Chen-Huang C, and McCrea RA.** Firing behavior of brain stem neurons during voluntary cancellation of the horizontal vestibuloocular reflex. II. Eye-movement related neurons. *J Neurophysiol* 70: 844–856, 1993.

**Cullen KE and Guitton D.** Analysis of primate IBN spike trains using system identification techniques. I. Relationship to eye movement dynamics during head-fixed saccades. *J Neurophysiol* 78: 3259–3282, 1997.

**Cullen KE, Rey CG, Guitton D, and Galiana HL.** The use of system identification techniques in the analysis of oculomotor burst neuron spike train dynamics. *J Comp Neurosci* 3: 347–368, 1996.

**Dichgans J, Bizzi E, Morasso P, and Tagliasco V.** Mechanisms underlying recovery of eye-head coordination following bilateral labyrinthectomy in monkeys. *Exp Brain Res* 18: 548–562, 1973.

**Dow RS.** Efferent connections of the flocculo-nodular lobe in *Macaca mulatta. J Comp Neurol* 68: 297–305, 1937.

**Dubrovsky AS and Cullen KE.** Gaze-, eye-, and head-movement dynamics during closed- and open-loop gaze pursuit. *J Neurophysiol* 87: 859–875, 2002.

**Eccles JC, Llinas R, and Sasaki K.** The excitatory synaptic action of climbing fibers on the Purkinje cells of the cerebellum. *J Physiol* 182: 268–296, 1996.

**Frens MA, Mathoera AL, and van der Steen J.** Floccular complex spike response to transparent retinal slip. *Neuron* 30: 795–801, 2001.

**Fuchs AF and Robinson DA.** A method for measuring horizontal and vertical eye movements in the monkey. *J Physiol* 191: 609–631, 1966.

**Fukushima K, Fukushima J, Kaneko CRS, and Fuchs AF.** Vertical Purkinje cells of the monkey floccular lobe: simple-spike activity during pursuit and passive whole body rotation. *J Neurophysiol* 82: 787–803, 1999.

**Fukushima K, Sato T, Fukushima J, Shinmei Y, and Kaneko CR.** Activity of smooth pursuit-related neurons in the monkey periarcuate cortex during pursuit and passive whole-body rotation. *J Neurophysiol* 83: 563–587, 2000.

**Gdowski GT and McCrea RA.** Integration of vestibular and head movement signals in the vestibular nuclei during whole-body rotation. *J Neurophysiol* 81: 436–449, 1999.

**Gdowski GT and McCrea RA.** Neck proprioceptive inputs to primate vestibular nucleus neurons. *Exp Brain Res* 135: 511–526, 2000.

**Gdowski GT, Belton T, and McCrea RA.** The neurophysiological substrate for the cervico-ocular reflex in the squirrel monkey. *Exp Brain Res* 140: 253–264, 2001.

**Gerrits NM and Voogd J.** The topographical organization of climbing and fossy fiber afferents in the flocculus and the ventral paraflocculus in rabbit, cat and monkey. *Exp Brain Res* 17: 26–29, 1989.

**Graf W, Simpson JI, and Leonard CS.** Spatial organization of visual messages of the rabbit's cerebellar flocculus. II. Complex and simple spike responses of Purkinje cells. *J Neurophysiol* 60: 2091–2121, 1988.

**Gresty M and Leech J.** Coordination of the head and eyes in pursuit of predictable and random target motion. *Aviat Space Environ Med* 48 :741–744, 1977.

**Hayes AV, Richmond BJ, and Optican LM.** A UNIX-based multiple process system for real time data acquisition and control. *WESCOM Conf Proc* 2: 1–10, 1982.

**Hirata Y and Highstein SM.** Acute adaptation of the vestibuloocular reflex: siganl processing by floccular and ventral paraflocular Purkinje cells. *J Neurophysiol* 85: 2267–2288, 2001.

**Huterer M and Cullen KE.** Vestibuloocular reflex dynamics during high-frequency and high-acceleration rotations of the head-on-body in rhesus monkey. *J Neurophysiol* 88: 13–28, 2002.

**Kato I, Watanabe S, Sato S, and Norita M.** Pretectofugal fibers from the nucleus of the optic tract in monkeys. *Brain Res* 705: 109–117, 1995.

**Kahlon M and Lisberger SG.** Changes in the responses of Purkinje cells in the floccular coplex of monkeys after motor learning in smooth pursuit eye movements. *J Neurophysiol* 84: 2945–2960, 2000.

**Kawano K, Sasaki M, and Yamashita M.** Response properties of neurons in posterior parietal cortex of monkey during visual-vestibular stimulation. I. Visual tracking neurons. *J Neurophysiol* 51: 340–351, 1984.

**Keller EL and Heinen SJ.** Generation of smooth-pursuit eye movements: neuronal mechanisms and pathways. *Neurosci Res* 11: 79–107, 1991.

**Komatsu H and Wurtz RH.** Relation of cortical areas MT and MST to pursuit eye movements. I. Localization and visual properties of neurons. *J Neurophysiol* 60: 580–603, 1988.

**Langer T, Fuchs AF, Chubb M, Scudder CA, and Lisberger SG.** Floccular efferents in the rhesus macaque as revealed by autoradiography and horseradish peroxidase. *J Comp Neurol* 235: 26–37, 1985.

**Lanman J, Bizzi E, and Allum J.** The coordination of eye and head movements during smooth pursuit. *Brain Res* 153: 39–53, 1978.

**Leung H-C, Suh M, and Kettner RE.** Cerebellar flocculus and paraflocculus Purkinje cell activity during circular pursuit in monkey. *J Neurophysiol* 83: 13–30, 2000.

**Lisberger SG.** Neural basis for motor learning in the vestibuloocular reflex of primates. III. Computational and behavioral analysis of the sites of learning. *J Neurophysiol* 72: 974–998, 1994.

**Lisberger SG and Fuchs AF.** Role of primate flocculus during rapid behavioral modification of vestibulo-ocular reflex. I. Purkinje cell activity during visually guided horizontal smooth pursuit eye movement and passive head rotation. *J Neurophysiol* 41: 733–763, 1978.

**Lisberger SG and Pavelko TA.** Brain stem neurons in modified pathways for motor learning in the primate vestibulo-ocular reflex. *Science* 242: 771–773, 1988.

**Lisberger SG, Pavelko TA, and Broussard DM.** Responses during eye movements of brain stem neurons that receive monosynaptic inhibition from the flocculus and ventral paraflocculus in monkeys. *J Neurophysiol* 72: 909–927, 1994a.

**Lisberger SG, Pavelko TA, and Broussard DM.** Neural basis for motor learning in the vestibuloocular reflex of primates. I. Changes in responses of brain stem neurons. *J Neurophysiol* 72: 928–953, 1994b.

**McCrea RA, Chen-Huang C, Belton T, and Gdowski GT.** Behavior contingent processing of vestibular sensory signals in the vestibular nuclei. *Ann NY Acad Sci* 781: 292–303, 1996.

**McCrea RA, Gdowski GT, Boyle R, and Belton T.** Firing behavior of vestibular neurons during active and passive head movements: vestibulospinal and other non-eye-movement related neurons. *J Neurophysiol* 82: 416–428, 1999.

**McCrea RA, Strassman A, May E, and Highstein SM.** Anatomical and physiological characteristics of vestibular neurons mediating the horizontal vestibule-ocular reflex of the squirrel monkey. *J Comp Neurol* 264: 547–570, 1987.

**McFarland JL and Fuchs AF.** Discharge patterns in nucleus hypoglossi and adjacent medial vestibular nucleus during horizontal eye movement in behaving macaques. *J Neurophysiol* 68 :319–332, 1992.

**Miles FA, Fuller JH, Braitman DJ, and Dow BM.** Long-term adaptive changes in primate vestibuloocular reflex. III. Electrophysiological observations in flocculus of normal monkey. *J Neurophysiol* 43: 1437–1476, 1980.

**Mustari MJ and Fuchs AF.** Response properties of single units in the lateral terminal nucleus of the accessory optic system in the behaving primate. *J Neurophysiol* 61: 1207–1220, 1989.

**Newsome WT, Wurtz RH, and Komatsu H.** Relation of cortical areas MT and MST to pursuit eye movements. II. Differentiation of retinal from extraretinal inputs. *J Neurophysiol* 60: 604–620, 1988.

**Noda H and Suzuki DA.** Processing of eye movement signals in the flocculus of the monkey. *J Physiol* 294: 349–364, 1979.

**Partsalis AM, Zhang Y, and Highstein SM.** Dorsal Y group in the squirrel monkey. II. Contribution of cerebellar flocculus to neuronal responses in normal and adapted animals. *J Neurophysiol* 73: 632–650, 1995.

**Rashbass C.** The relationship between saccadic and smooth tracking eye movements. *J Physiol* 159: 326–338, 1961.

**Raymond JL and Lisberger SG.** Multiple subclasses of Purkinje cells in the primate floccular complex provide similar signals to guide learning in the vestibulo-ocular reflex. *Learn Mem* 3: 503–518, 1997.

**Raymond JL and Lisberger SG.** Neural learning rules for the vestibulo-ocular reflex. *J Neurosci* 18: 9112–9129, 1998.

**Roy JE and Cullen KE.** Selective processing of vestibular reafference during self-generated head motion. *J Neurosci* 21: 2131–2142, 2001.

**Roy JE and Cullen KE.** Vestibuloocular reflex signal modulation during voluntary and passive head movements. *J Neurophysiol* 87: 2337–2357, 2002.

**Sakata H, Shibutani H, and Kawano K.** Functional properties of visual tracking neurons in posterior parietal associated cortex of the monkey. *J Neurophysiol* 49: 1369–1380, 1983.

**Sato H, Ohkawa T, Uchino Y, and Wilson VJ.** Excitatory connections between neurons of the central cervical nucleus and vestibular neurons in the cat. *Exp Brain Res* 115: 381–386, 1997.

**Scudder CA and Fuchs AF.** Physiological and behavioral identification of vestibular nucleus neurons mediating the horizontal vestibuloocular reflex in trained rhesus monkeys. *J Neurophysiol* 68: 244–264, 1992.

**Simpson JI, Wylie DR, and De Zeeuw CI.** On climbing fiber signals and their consequence(s). *Behav Brain Sci* 19: 384–398, 1996.

**Stone LS and Lisberger SG.** Visual responses of Purkinje cells in the cerebellar flocculus during smooth-pursuit eye movements in monkeys. I. Simple spikes. *J Neurophysiol* 63: 1241–1261, 1990a.

**Stone LS and Lisberger SG.** Visual responses of Purkinje cells in the cerebellar flocculus during smooth-pursuit eye movements in monkeys. II. Complex spikes. *J Neurophysiol* 63: 1262–1275, 1990b.

**Suh M, Leung H-C, and Kettner RE.** Cerebellar flocculus and ventral paraflocculus Purkinje cellactivity during predictive and visually driven pursuit in monkey. *J Neurophysiol* 84: 1835–1850, 2000.

**Sylvestre PA and Cullen KE.** Quantitative analysis of abducens neuron discharge dynamics during saccadic and slow eye movements. *J Neurophysiol* 82: 2616–2632, 1999.

**Tanaka M and Fukushima K.** Neuronal responses related to smooth pursuit eye movements in the periarcuate cortical area of monkeys. *J Neurophysiol* 80: 28–47, 1998.

**Thach WT.** Somatosensory receptive fields of single units in the cat cerebellar cortex. *J Neurophysiol* 30: 1–22, 1995.

**Tomlinson RD and Robinson DA.** Signals in vestibular nucleus mediating vertical eye movements in monkey. *J Neurophysiol* 51: 1121–1136, 1984.

**Waterston JA, Barnes GB, and Grealy MA.** A quantitative study of eye and head movements during smooth pursuit in patients with cerebellar disease. *Brain* 115: 1343–1358, 1992.

**Wellenius GA and Cullen KE.** A comparison of head-unrestrained and head-restrained pursuit: influence of eye position and target velocity on latency. *Exp Brain Res* 133: 139–155, 2000.

**Wilson VJ, Yamagata Y, Yates BJ, Schor RH, and Nonaka S.** Response of vestibular neurons to head rotations in vertical planes. III. Response of vestibulocollic neurons to vestibular and neck stimulation. *J Neurophysiol* 64: 1695–1703, 1990.

**Wylie DRW and Linkenhoker B.** Mossy fibers from the nucleus of the basal optic root project to the vestibular and cerebellar nuclei in pigeons. *Neurosci Lett* 219: 83–86, 1996.

**Yakushin SB, Gizzi M, Reisine H, Raphan, Büttner-Ennever J, and Cohen B.** Functions of the nucleus of the optic tract (NOT). II. Control of ocular pursuit. *Exp Brain Res* 131: 433–447, 2000.

**Zhang Y, Partsalis AG, and Highstein SM.** Properties of superior vestibular nucleus flocculus target neurons in the squirrel monkey. I. General properties in comparison with flocculus projecting neurons. *J Neurophysiol* 73: 2261–2278, 1995a.

**Zhang Y, Partsalis AG, and Highstein SM.** Properties of superior vestibular nucleus flocculus target neurons in the squirrel monkey. II. Signal components revealed by reversible flocculus inactivation. *J Neurophysiol* 73: 2279–2292, 1995b.